Sustainable Processes Connect
ISSN: 3079-1421
2026, Article ID. 2026.0024, Cite as: https://doi.org/10.69709/SusProc.2026.171930

SCIFINITI PUBLISHING

Review Article

OPEN ACCESS

Plant-Mediated Green Synthesis of Nanomaterials for Sustainable Energy Applications

Sana Khan[1] Tripti Singh[1,*] Prachi Sharma[2] Bhumika Vishnoi[1] Gunjan Sharma[1] Deepti Singh[3] Shambhavi Roy[4]

[1] Institute of Management Studies, Ghaziabad (University Course Campus), NH 09, Adhyatmik Nagar, Ghaziabad 201015, India
[2] JMS Institute of Technology (JMS IT), Ghaziabad, Ghaziabad 201015, Uttar Pradesh, India
[3] Amity Institute of Biotechnology, Amity University, Uttar Pradesh, Sector- 125, Noida 201313, Uttar Pradesh, India
[4] Manipal School of Life Sciences, Manipal Academy of Higher Education, Manipal 576104, India

Article History
Received: September 03, 2025 Accepted: March 23, 2026 Published: May 11, 2026

Abstract
Nanoparticles synthesized via physical or chemical methods can pose significant environmental risks due to their inherent toxicity. Consequently, the green synthesis of nanoparticles using plant extracts has emerged as a safer and more sustainable alternative. This paper focuses on the plant-mediated synthesis of various nanoscale metal particles (Ag, Au, Cu), metal oxide nanoparticles (ZnO, TiO_2, Fe_3O_4), and carbon-based nanomaterials, including carbon nanotubes, quantum dots, and graphene. Plant phytochemicals, including polysaccharides, flavonoids, enzymes, reducing sugars, steroids, proteins, terpenoids, and amino acids, play a crucial role in the stabilization, capping, and reduction processes during nanoparticle biosynthesis. Factors such as pH, extract concentration, reaction temperature, metal salt concentration, contact time, and the ratio of plant extract to metal salt are discussed. Beyond biomedical and catalytic applications, this paper highlights the significance of green nanoparticles for the production of biofuels. Despite significant advancements, plant-mediated green nanotechnology requires further development before it can be fully established as a climate-resilient and sustainable solution for meeting the energy demands of a growing global population. To address the pressing issue of fuel depletion, sustained research efforts and careful long-term implementation are required.

Keywords:
green nanotechnology; biofuel production; plant mediated synthesis; metal nanoparticles; carbon nanomaterials

1. Introduction

The domain of nanotechnology has proven to be one of the most rapidly evolving and dynamic areas of research [1]. This scientific domain primarily focuses on the synthesis, development, structural characterization, and applications of nanomaterials, which typically range in size from 1 to 100 nm. Nanomaterials are generally classified into four categories based on their dimensionality. Zero-dimensional (0D) nanomaterials include those in which all dimensions fall within the nanoscale range, such as fullerenes, nanoparticles, and quantum dots. One-dimensional (1D) nanomaterials include those in which only one dimension extends beyond the nanoscale range, such as nanorods, nanohorns, nanotubes, nanowires, and nanofibers. Two-dimensional (2D) nanomaterials are nanostructures in which two dimensions extend beyond the nanoscale range, including nanolayers, nanosheets, and nanofilms. Three-dimensional (3D) nanomaterials are those in which all dimensions extend beyond the nanoscale range, such as bulk powders and arrays of nanowires [2]. Supplementary Table S1 summarizes this dimensional classification along with representative examples and their key structural characteristics [3–6].

Over the past decade, nanomaterials, particularly nanoparticles, have been extensively explored due to their unique properties [7]. Nanoparticles exhibit diverse properties, including unique biological interactions, mechanical stability, steric stabilization, thermal and electrical conductivity, and altered fusion temperature, compared with

* **Corresponding Author:**
Tripti Singh, Institute of Management Studies, Ghaziabad (University Course Campus), NH 09, Adhyatmik Nagar, Ghaziabad 201015, India, drtriptisingh@imsuc.ac.in

their bulk counterparts, owing to their small size and increased surface area per unit mass [8]. The synthesis of nanoparticles has attracted significant interest among researchers due to their wide-ranging applications in medicine, photonics, biotechnology, biofuel production, cosmetics, electronics, drug and gene delivery, catalysis, nonlinear optical devices, and the chemical industry [9,10].

The literature reports a variety of chemical, physical, and biological approaches for the synthesis of different categories of nanoscale particles. Figure 1 illustrates the major nanoparticle synthesis methods, highlighting the biological routes through plants and microbes [1]. Nanoparticle fabrication through physical methods typically follows a top-down approach, in which bulk materials are broken down into nanoscale structures. These methods include laser ablation, inert gas condensation (IGC), laser pyrolysis, and electrospinning [11], whereas chemical methods (e.g., etching, chemical vapor deposition, and the sol-gel method) and biological (green) synthesis methods employ a bottom-up approach involving the assembly of atoms or molecules into nanomaterials [12]. However, physical and chemical methods may contribute to environmental toxicity and related problems. They are accompanied by several limitations such as prolonged synthesis time, high production cost and complex purification steps [13]. Some physical methods (e.g., tube furnace processes) require substantial energy input to maintain high operating temperatures, which can increase processing time because thermal stability must be achieved. In contrast, chemical techniques often involve hazardous reducing agents such as borohydride, hydrazine hydrate, and formaldehyde, which restrict their applicability in pharmaceutical and clinical fields [14]. In contrast, green synthesis approaches offer a more sustainable and environmentally friendly alternative. These methods minimize the use of toxic chemicals, reduce energy consumption, and enhance cost-effectiveness compared to conventional techniques [1,10,13–15].

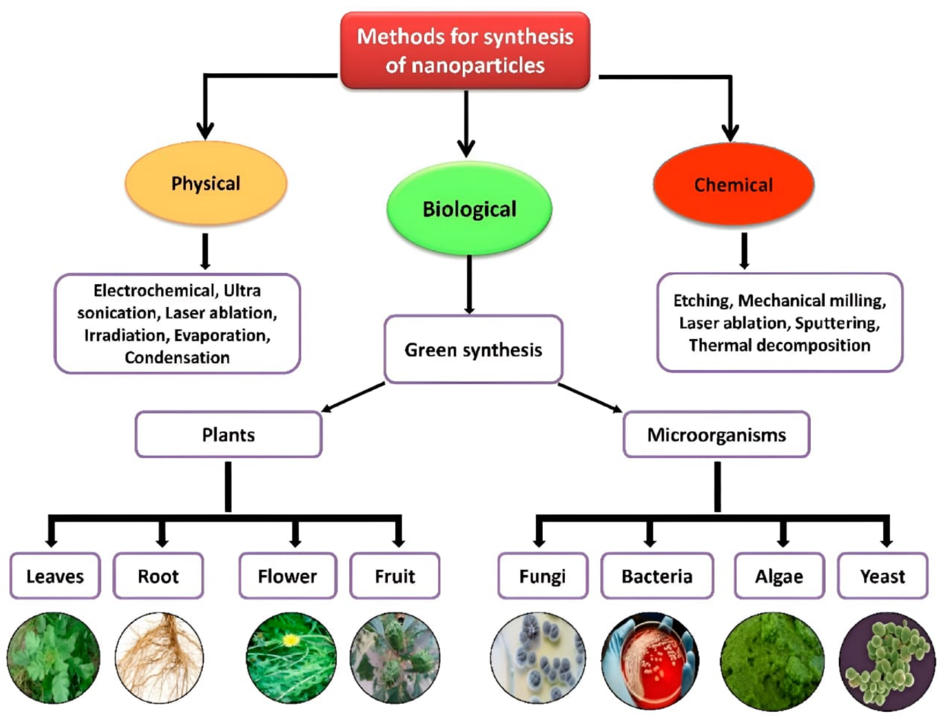

Figure 1: Overview of physical, chemical, and biological methods for nanoparticle synthesis, highlighting the comparative advantages of eco-friendly biological routes. The diagram emphasizes the growing preference for plant-mediated synthesis due to its simplicity, cost-effectiveness, and reduced environmental impact. (Adapted from Khan et al. 2022 [1], licensed under CC BY 4.0.).

Researchers have recognized the urgent need to minimize the use of harmful chemicals and reduce energy consumption, shifting toward biological methods for nanoparticle synthesis that utilize natural reducing, capping, and stabilizing agents. Numerous biological agents, including microbes (molds, unicellular fungi, algae, and bacteria), agricultural wastes, and plants (leaves, stems, fruits, roots, flowers, bark, and seeds), have been extensively investigated for facilitating environmentally friendly synthesis [16]. Several studies suggest that microbes have a short growth period and are relatively easy to manage, making them suitable for the synthesis of specific nanoparticles [17]. However, plant extracts are considered more efficient, as scaling up microbial preparations is challenging and can reduce the production rate [10,18]. Plants are capable of reducing metal ions significantly faster than microbes [18]. It is widely recognized that plant-derived nanoparticles limit the use of hazardous and toxic residues compared to chemically synthesized nanoparticles, and can be safely applied in agriculture, food science and technology, public health, and biomedical engineering. Various biomolecules present in plants, such as coenzymes, carbohydrates, phenolic acids, amino acids, alkaloids, gums, flavonoids, polysaccharides, steroids, vitamins, tannins, proteins, fats, terpenoids, and alcohols, possess reducing capabilities and can convert inorganic metal ions into metal nanoparticles [10].

This paper specifically highlights the use of plants as a sustainable source for the production of various metal (Au, Ag) and metal oxide nanoparticles (ZnO, TiO_2) through environmentally friendly green synthesis, as well as their significant potential in photocatalysis and biofuel production [8]. These plant-derived nanoparticles have shown promising roles in biofuel systems, particularly as catalysts in transesterification and biomass-conversion reactions and as enhancers of microalgal lipid accumulation and biodiesel yield [19,20]. This paper also discusses the advantages of the green synthesis of nanoparticles over conventional chemical and physical methods.

2. Synthesis of NPs from Plants

2.1. Role of Plant Metabolites in Nanoparticle Synthesis

Crude plant extracts contain a wide variety of primary and secondary metabolites. Primary metabolites include carbohydrates, proteins, fatty acids, nucleic acids, and amino acids, which play essential roles in plant growth and development. In contrast, secondary metabolites are produced by plants only under specific stress conditions. These include phenolic acids, flavonoids, alkaloids, terpenoids, alcohols, antioxidants, organic acids (e.g., oxalic acid, ascorbic acid, and tartaric acid), and quinones [21]. Although secondary metabolites do not directly influence plant growth or development, they are ecologically important and have demonstrated significant potential in medicinal applications, including both traditional and modern medicine. Owing to the wide variety of metabolites present in plants, it is challenging to identify a specific compound responsible for the formation of metallic nanoparticles. Hence, various metabolites, including flavonoids, phenolic acids, terpenoids, and proteins, have been reported to facilitate the synthesis of nanoparticles due to their reducing and stabilizing capabilities throughout the biosynthesis process [22]. These metabolites mediate the reduction of metal ions, resulting in nanoparticle formation through a one-step, environmentally friendly synthesis method [23,24]. Figure 2 demonstrates the typical mechanism of silver nanoparticle formation involving reduction and capping by plant-derived metabolites [25]. Several metabolites act as precursors during the green synthesis of plant-mediated nanoparticles. They offer numerous advantages over chemical methods, making them suitable for applications in medicinal and pharmaceutical fields. Additionally, they are cost-effective and readily available. Biomolecules that serve as reducing and stabilizing agents include sugars, ketones, aldehydes, and carboxylic acids [26].

2.1.1. Phenolics

Phenolic acids belong to the polyphenol family, the most abundant class of secondary metabolites produced by plants. These compounds are biosynthesized via either the polyketide acetate/malonate pathway, which generates simple phenols, or the shikimate/phenylpropanoid pathway, which produces phenylpropanoids.

Gopinath et al. synthesized silver, gold, and silver–gold bimetallic nanoparticles using leaf extracts of *Gloriosa superba*. These nanoparticles were characterized using X-ray diffraction (XRD), Fourier-transform infrared (FTIR) spectroscopy, ultraviolet–visible (UV-Vis) spectroscopy, atomic force microscopy (AFM), and transmission electron microscopy (TEM). They reported that sugar-derived compounds, such as glycosides and hydrophilic tannins present in the leaves, facilitated the bioreduction of $AgNO_3$, $HAuCl_4{\cdot}3H_2O$, and their 1:1 mixture into silver, gold, and silver–gold bimetallic nanoparticles. This process could be visually monitored by the color changes, from colorless to brown, yellowish white to reddish brown, and yellow to dark red, indicating the successful formation of silver, silver gold bimetallic, and gold nanoparticles [27]. Hemlata et al. (2020) used the aqueous leaf extract of *Cucumis prophetarum* for the green synthesis of silver-based nanostructures. Further analysis of the bioactive compounds in the leaf extract revealed the presence of triterpenoids, phenols, tannins, and saponins, which played a key role in reducing and capping the nanoparticles to maintain their stability and prevent aggregation [28]. Numerous phenolic acids, such as caffeic acid and ellagic acid, act as reducing agents to facilitate the formation of metal nanoparticles.

The molecular framework of phenolics includes a phenolic ring and, in some cases, a carboxylic acid group. The aromatic ring plays a key role in antioxidant activity and metal chelation [10]. Wang et al. (2014) demonstrated that polyphenols, in combination with charged iron particles, produce complex nanoparticles with a size range of 50–90 nm. They utilized leaf extracts from three plants in their study, namely *Melaleuca nesophila, Rosmarinus officinalis*, and *Eucalyptus tereticornis* [29].

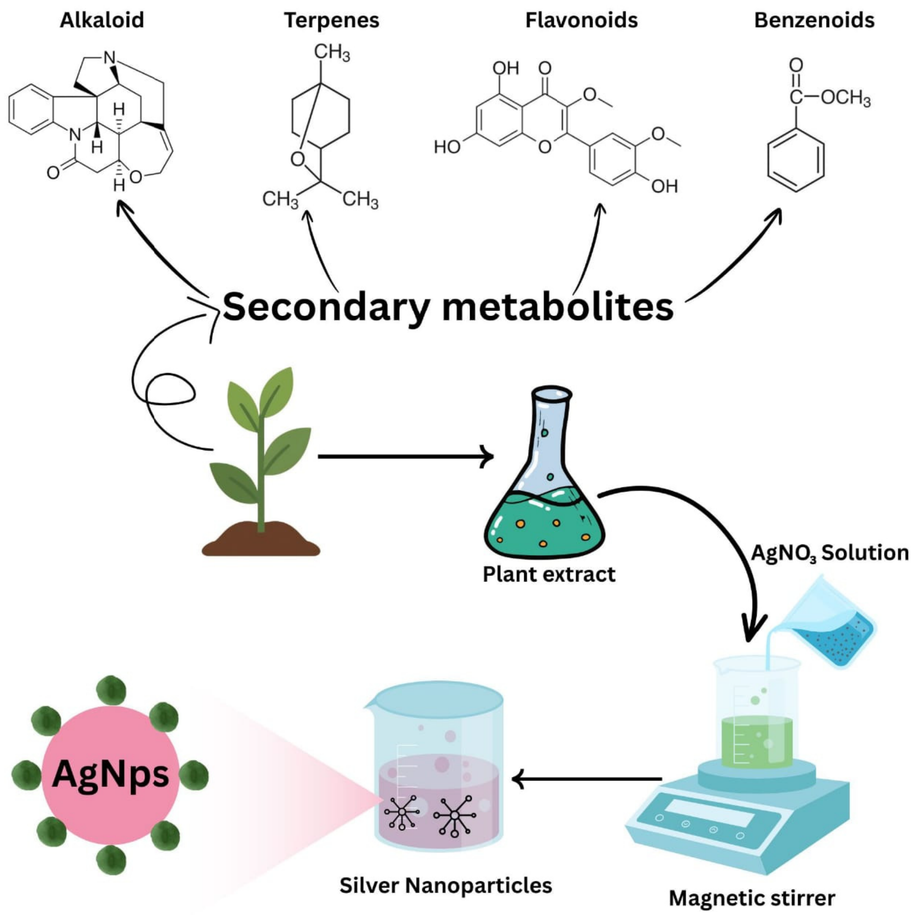

Figure 2: Proposed mechanism of silver nanoparticles (AgNPs) synthesis mediated by plant extracts. The figure illustrates the involvement of plant-derived secondary metabolites, including alkaloids, terpenes, flavonoids, and benzenoids, in the synthesis and stabilization of silver nanoparticles through the green synthesis approach.

2.1.2. Flavonoids

Flavonoids, a class of secondary metabolites, are considered primary reducing agents in the green synthesis of metal nanoparticles. To date, 7000 compounds from this family have been reported. They have low molecular weight and, structurally, consist of 15 carbon atoms with two aromatic rings (A and B) connected by a three-carbon bridge (C). They can be found as flavan-3-ols, flavones, flavanols, isoflavones, flavanones, and anthocyanidins. In plants, they are present as glycosides or methylated derivatives [22].

Flavonoids are biosynthesized via the phenylpropanoid metabolic pathway, which begins with the conversion of phenylalanine into 4-coumaroyl-CoA. The enzyme chalcone synthase catalyzes the formation of chalcone scaffolds from 4-coumaroyl-CoA, which serves as the backbone for all flavonoids [30]. Various flavonoid subclasses arise through the action of different enzymes, including hydroxylases, reductases, Fe^{2+}/2-oxoglutarate-dependent dioxygenases, and isomerases, which modify the structural framework of flavonoids [31].

Various studies have been reported in the literature regarding their ability to act as reductants, which is mainly due to their ability to donate electrons and 'H' atoms [10]. Sahu et al. (2016) demonstrated the production of silver nanoparticles (AgNPs) using a range of flavonoids, including hesperidin, naringin, and diosmin, to reduce Ag^+ ions. Additionally, these flavonoids were also found to function as capping agents, thereby influencing the antimicrobial effects of AgNPs [32]. Bose and Chatterjee (2016) reduced Ag^+ ions to silver nanoparticles using leaf decoction from Psidium guajava (guava plant). The authors suggested that quercetin (a flavonoid) reduces Ag^+ to Ag^0 by liberating Hydrogen and is oxidized to form a quinone. The hydroxyl and oxo functional groups of quercetin molecules subsequently act as capping agents, stabilizing the silver nanoparticles [33]. Melkamu and Bitew (2021) reported the eco-friendly synthesis of silver nanoparticles utilizing the leaf extract from the *Hagenia abyssinica* plant. The phytochemical evaluation of the leaf extract indicated the presence of compounds such as anthraquinones, saponins, tannins, alkaloids, phenols, and flavonoids, which contributed to the reduction, capping, and stabilization of nanoparticles throughout this process. The interaction of flavonoids with metal ions through carbonyl functional groups releases hydrogen, converting the enol form of flavonoids into the keto form, which facilitates the formation of Ag^0 [34].

2.1.3. Terpenoids

Terpenoids are commonly obtained from the essential oils of plants, with approximately 90% of these oils consisting of terpenoids, which are oxygenated terpenes [22].

The typical formula for terpenoids is (C5H8) n, with 'n' indicating the number of isoprene units in the compound. On the basis of number of n, terpenoids can be classified into: hemiterpene (n = 1, C5), monoterpene (n = 2, C10), sesquiterpene (n = 3, C15), diterpene (n = 4, C20), sesterpene (n = 5, C25), triterpene (n = 6, C30), tetraterpene (n = 8, C40) and polyterpene [35].

The biosynthesis of terpenoids mainly occurs through two pathways: the mevalonate (MVA) pathway ... and the 2C-methyl-D-erythritol-4-phosphate (MEP) pathway, which takes place in the plastid. Both these pathways lead to the production of isopentenyl pyrophosphate (IPP) and dimethylallyl pyrophosphate (DMAPP). DMAPP and IPP serve as building blocks for the synthesis of geranyl pyrophosphate (GPP), a 10-carbon molecule that gives rise to monoterpenes. On further addition of IPP units, a 15-carbon molecule, Farnesyl pyrophosphate (FPP), and geranylgeranyl pyrophosphate (GGPP), a 20-carbon molecule, are produced, which give rise to sesquiterpenes and diterpenes, respectively [36]. These sesquiterpenes and monoterpenes are recognized as playing a crucial role in the production of silver nanoparticles [37]. They act as surface-active agents to stabilize and reduce nanoparticles; however, their exact mechanism remains unclear. Shankar et al. reduced silver ions into nanoparticles by using geranium leaves extract to demonstrate the role of terpenoids in the biosynthesis of nanoparticles [38]. Pungle et al. (2022) demonstrated the eco-friendly synthesis of silver nanoparticles using aqueous leaf extracts of *Tridax procumbens*. FTIR analysis of the leaf solution showed the presence of amines and hydroxyl groups in combination with fluoro compounds. Upon further analysis by HRLC-MS, the major capping agent was found to be fusinopril, and reducing agents were found to be peptides, terpenoids, polyphenols, and alkaloids [39]. According to Ahmed et al. (2010), eugenol plays a key role in the bioreduction process during the synthesis of silver and gold nanoparticles from extracts of *C. zeylanicum* [40].

Scientists have suggested that the phenolic OH bond of eugenol undergoes homolytic cleavage in the presence of sunlight, releasing H^+ ions that reduce Ag^+ to Ag^0 [41].

2.1.4. Proteins

Proteins act as reducing agents by donating electrons to metallic ions during the plant-mediated green synthesis of nanoscale particles. Mukherjee et al. performed SDS-PAGE analysis of leaf extracts of Olax scandens and the concentrated supernatant of silver nanoparticles derived from this extract. The results indicated the presence of low-molecular-weight proteins in the leaf extracts; however, no such proteins were detected in the newly synthesized nanoparticles. This suggests the utilization of low-molecular-weight proteins during nanoparticle biosynthesis [42]. Shukla et al. (2008) demonstrated the production of gold nanoparticles derived from soybeans by directly mixing soybeans with sodium tetrachloroaurate ($NaAuCl_4$) in an aqueous medium. To investigate the role of soybean proteins in the reduction of sodium tetrachloroaurate ($NaAuCl_4$), the proteins were separated into low-molecular-mass (<5 kDa) and high-molecular-mass (>5 kDa) fractions using Centricon Plus-20 centrifugal filtration devices. Both protein fractions were then separately mixed with sodium tetrachloroaurate ($NaAuCl_4$) in an aqueous medium, and each fraction successfully facilitated the formation of gold nanoparticles, thereby confirming their role as key reducing agents in the process [43].

Tavaf et al. (2015) effectively utilized reduced glycated adducts of the whole casein fraction as both reducing and stabilizing agents in the synthesis of silver nanoparticles [44]. Using FTIR spectroscopy, a variety of C=O groups present in proteins have been proven to act as capping ligands. They associate with the nanoparticle surface, contributing to colloidal stability. Additionally, proteins and amino acids containing exposed disulfide bonds and thiol groups act as both reducing and stabilizing agents during the biosynthesis of nanoscale particles [41]. Bhattacharjee et al. (2005) generated gold nanoparticles using a tripeptide sequence featuring an exposed N-terminal group [45].

3. Mechanism of Plant-Derived Nanoparticles

The application of green chemistry in nanoparticle synthesis has been extensively explored in recent years. This green synthesis relies on a bottom-up approach, in which nanoparticles are assembled from smaller precursor entities. Unlike conventional synthesis methods, plant-mediated synthesis typically requires only an aqueous extract, ambient temperature, and atmospheric pressure, thereby minimizing energy consumption [46]. However, careful consideration of the solvent type is essential, with water and ethanol being the most commonly employed due to their effectiveness in extracting phytochemicals and maintaining their stability, as well as their low environmental impact [47,48]. Lee et al. (2024) demonstrated that ethanol and water extracts effectively recover antioxidant and phenolic compounds, offering lower safety risks compared with more toxic organic solvents such as methanol [49]. Nortjie et al. (2022) further emphasized that an ideal extraction solvent should possess low toxicity, suitable volatility, strong solubility for target compounds, and the ability to evaporate readily at mild temperatures. Accordingly, the selection of solvents such as water or ethanol, which meet these criteria and present minimal environmental and health hazards, is preferred in green synthesis approaches [47]. Compared with conventional chemical nanoparticle syntheses that often employ strong reductants (e.g., NaBH4, hydrazine) and hazardous surfactants/solvents, the plant-based (green) approach generally reduces the use of highly toxic reagents and associated toxic by-products [50,51].

The essential tools, processes, and materials used in nanoparticle synthesis encompass reductants, stabilizers, solvents, metal precursors, nucleation, growth, aggregation, stabilization, and characterization [1]. Plant-based nanoparticle synthesis has emerged as a more favorable approach for large-scale industrial applications due to its minimal environmental impact and economic advantages, as it is relatively cost-effective to scale up [23]. A systematic approach is required for plant-mediated nanoparticle synthesis, which can be described as follows:

1) The plant should be taxonomically identified, and the specific plant material should be carefully selected.
2) The extraction process is carried out using appropriate solvent(s), followed by filtration to minimize the risk of introducing impurities.
3) A metal salt solution is used as a nanoparticle precursor and is mixed with the plant extract.
4) Controlling physical factors (such as pH, temperature, phytochemical concentration, and metal salt concentration) is necessary to ensure a successful reaction.
5) The nanoparticle formation is signified by a change in the solution's color.
6) Centrifugation is then carried out to separate the nanoparticles from the solution and remove any remaining impurities.
7) Finally, the synthesized nanoparticles are characterized using a range of analytical techniques to determine their size, shape, composition, and physicochemical properties [10].

The eco-friendly synthesis of plant-derived nanoparticles can be summarized in three primary stages: (1) the activation phase, (2) the growth phase, and (3) the termination phase:

- The Activation Phase

Plant metabolites play a crucial role in reducing metal ions from their respective salt precursors during the activation phase. Researchers have reported that each metal exhibits different reductive capabilities, which directly influence the reduction of metal ions or their precursors during the green synthesis process. In addition, the oxidation state of metal ions changes from monovalent or divalent forms to the zero-valent state, and the reduced metal atoms subsequently undergo nucleation [52]. It represents the initial stage of nanoparticle formation in plant-mediated green synthesis. Nucleation leads to the formation of clusters, which are referred to as nuclei in wet-chemical nanoparticle synthesis. The radius of these clusters corresponds to the minimum size at which a particle can remain stable in the solution without redissolving into it. This process is essential for the formation of stable clusters, which, upon growth, give rise to nanoparticles [53].

- The Growth Phase

The growth phase follows a bottom-up approach and primarily depends on the interaction between stable nuclei and surfactants. The length and chemical nature of the surfactant should also be taken into consideration. Several studies suggest that surfactant–solvent interactions can in-

2026, Vol. 2, Article ID. 2026.0024
https://doi.org/10.69709/SusProc.2026.171930

fluence the size and structural characteristics of nanoparticles. Additionally, it was experimentally demonstrated that stable nuclei are observed at low surfactant concentrations. In contrast, nucleation and growth processes are inhibited in the presence of an excess of a strongly binding surfactant [53].

As the growth phase progresses, smaller nanoparticles aggregate to form nanotubes, nanotriangles, nanoprisms, and various other irregular morphologies until thermodynamic stability is reached. This thermodynamic process is known as Ostwald ripening [54].

- The Termination Phase

When the nanoparticles acquire the most energetically favorable conformation and attain a constant size and shape, the process terminates. The lower the Gibbs free energy of a nanoparticle, the greater its stability. This phase is highly dependent on plant extracts, which act to stabilize the nanoparticles. Based on FTIR analysis, certain plant functional moieties, such as —C—O—C—, —C=C—, and —C=O, were observed to act as protective stabilizers, thereby aiding nanoparticle stabilization and preventing further changes in their morphology [54]. The schematic in Figure 3 illustrates a typical synthesis procedure using zinc acetate and strawberry extract, highlighting the role of phytochemicals in the reduction process, Ostwald ripening, and stabilization stages under controlled temperature and stirring conditions.

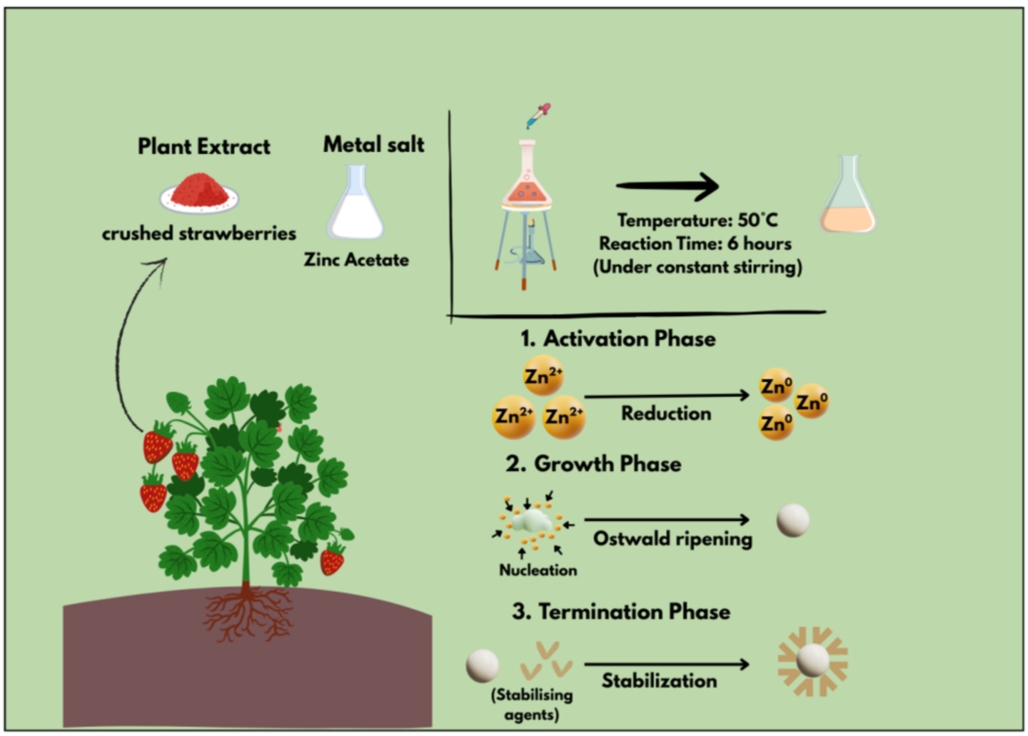

Figure 3: Schematic representation of the green synthesis of ZnO nanoparticles using crushed strawberry fruit extract as a reducing and stabilizing agent. The process demonstrates how plant-derived biomolecules contribute to the controlled formation of ZnO nanoparticles with enhanced biocompatibility and catalytic potential.

4. Factors Affecting Plant-Mediated Synthesis of Nanoparticles

Apart from phytochemical factors, various physicochemical parameters such as temperature, contact time, reaction environment, concentration, pH, plant extract composition, metal precursor concentration, particle size of the raw materials, plant part used, the ratio of plant extract to metal solution, and catalyst activity play a crucial role in determining the shape and size of nanoparticles. In many cases, these factors also play a crucial role in determining the application range of the resulting nanoscale particles [10]. Therefore, it is essential to control these factors during the biosynthesis of nanoparticles to ensure monodispersity, stability, controlled morphology, synthesis rate, and scalability of production. The optimum value of these factors was determined by studying one factor at a time for different values while keeping the other factors constant. During experimental design, these factors are carefully selected to obtain smaller-sized nanoparticles [46]. It should also be noted that the phytochemical composition of plant extracts can vary with factors such as season, geographic locations, growth conditions, and use of fertilizers and pesticides, which may lead to inconsistencies in nanoparticle size, shape, and yield [14,55]. Additionally, the standardization of extract preparation remains difficult, affecting reproducibility and large-scale production [56].

Supplementary Table S2 summarizes the principal factors reported in previous studies, outlining how each condition influences nanoparticle characteristics such as size, shape, and stability [1,8,57].

4.1. pH

Numerous studies have demonstrated the significant influence of pH on the biosynthesis of nanoparticles. pH can influence the electrical charge of metabolites involved in nanoparticle synthesis, thereby affecting their size and morphology [58]. Muthu et al. (2017) investigated the influence of pH on the synthesis of silver nanoparticles using the flower extract of *Cassia auriculata* [59]. Rajput et al. (2020) reported that a neutral pH (7) at 60 ± 2 °C resulted in the formation of small, spherical silver nanoparticles, with sizes ranging from 5 to 20 nm, using leaf extracts of Indian belladonna. They observed that the peak intensity in the UV–Vis spectrum of silver nanoparticles increased as the pH was raised from 3 to 11, with a higher reaction rate under alkaline conditions. However, alkaline pH also led to the formation of larger silver nanoparticles. Hence, a balanced pH level (7) was marked as the optimum pH to derive silver nanoparticles [58]. Miranda et al. (2022) showed how pH influences the size, shape, and antimicrobial characteristics of silver nanoparticles derived from a leaf-sourced extract of *Spinacia oleracea*. They highlighted the importance of pH by reporting that only those silver nanoparticles synthesized at pH 4, 5, and 9 had antimicrobial activity against *Candida albicans* and *Escherichia coli*. They conducted their experiments over a pH range of 5–9 and observed that particle size decreased as pH increased. The smallest silver nanoparticles were obtained at pH 8, with a particle size of 91.75 nm, whereas the particle size increased to 263.6 nm at pH 9. Upon TEM analysis, silver nanoparticles synthesized at pH 8 appeared spherical with rough surfaces. However, silver nanoparticles synthesized without pH adjustment exhibited both rod-like and spherical morphologies. Additionally, the stability of the silver nanoparticles was evaluated by storing them for 8 weeks, followed by re-assessment of their antimicrobial activity against the aforementioned microorganisms. Only the nanoparticles synthesized at pH 4 and 5 retained their antimicrobial effectiveness, whereas those produced at pH 9 showed reduced activity [60].

Jeevanandam et al. (2019) reported a study demonstrating the morphological transformation of MgO nanoparticles upon changes in pH. They prepared MgO nanoparticles using leaf extract of *Amaranthus tricolor* at 60 °C and neutral pH (7) for 10 min. They observed that the solution color changed from pale red to yellow when the pH was adjusted to alkaline conditions (pH 9 and 11). Moreover, neutral pH (7) led to the formation of spherical MgO nanoparticles, which transformed into hexagonal structures upon decreasing the pH through the addition of hydrogen ions. Their morphological characteristics were validated through TEM analysis [61]. Lee et al. (2019), also reported that nanosilver particles synthesized using fruit peel-derived extract from *Garcinia mangostana* at pH 4 had a spherical shape with an average diameter of 32.7 nm, which reduced to 7.12 nm when the pH was adjusted to 7 [62]. In 2021, Amjad et al. reported that an acidic medium (pH 5.5) favored the maximum production of copper nanoparticles compared to a basic medium (pH 7.5) during the green synthesis using leaf extract of *F. margarita* [63].

Coman et al. (2024) highlighted the role of pH in the synthesis of platinum nanoparticles and experimentally concluded that maintaining an optimal pH is essential for efficient and faster reaction progression. They set the pH at 7.5, 8, 9, and 10 while synthesizing platinum nanoparticles and found that *Quercus dalechampii* and *Quercus frainetto* contributed most efficiently to the formation of platinum nanoparticles at pH 10, whereas pH 9 supported the most efficient formation of platinum nanoparticles using *Quercus petraea* [64]. Imade et al. (2022) reported the fabrication of zinc oxide nanoparticles using a plantain peel-derived extract, in which the reaction pH was adjusted to 12 to facilitate efficient nanoparticle synthesis [65]. In a similar study, Al Awadh et al. (2022) investigated the effect of different pH levels on the synthesis of ZnO nanoparticles using leaf extract of *Raphanus sativus*. They observed a characteristic absorption peak at pH 10 and 11, whereas no such peak was detected at higher pH values (12–14). Based on these findings, they identified pH 10 as the optimal reaction condition [66]. In a recent study conducted by Hirphaye et al., the researchers noted that a pH of 12 was highly effective in forming MgO nanoparticles from the female flower of *Hagenia abyssinica* [67]. A lower absorbance peak was observed when the pH was adjusted from 2 to 10, indicating poor nanoparticle formation.

4.2. Temperature

Temperature is another factor that influences the morphology and dimensions of nanoparticles. Many studies have reported that temperature exhibits an inverse relationship with nanoparticle size, where increasing temperature generally leads to the formation of smaller nanoparticles. Lee et al. (2019) investigated the effect of temperature on the formation of silver nanoparticles synthesized using *Garcinia mangostana* fruit peel extract. They found that at room temperature (27 °C), the nanoparticles exhibited an irregular spherical morphology with a mean diameter of 49.91 nm. However, when the temperature was increased to 45 °C, the nanoparticles became more uniformly spherical, and their size decreased to 33.61 nm [62]. Khalil et al. (2013), also reported a similar study [68]. Rajput et al. (2020), recorded the formation of silver nanoparticles at various temperatures, including 20 °C, 40 °C, 60 °C, and 80 °C. Upon the green synthesis of silver nanoparticles using leaf extract of Atropa acuminata at pH 7 for 30 min, it was observed that the bioreduction of silver ions increased at higher temperatures, resulting in smaller nanoparticles. Accordingly, 60 °C was identified as the optimum temperature for the synthesis of silver nanoparticles [58]. Zheng et al. noted that the rate of reduction of platinum (II) ions was much higher at 90 °C than that observed at 30 °C and 60 °C. Herein, the smaller particle size was attributed to an insufficient Pt^0 source; therefore, 90 °C was identified as the optimal temperature [69].

Ansari et al. (2023) synthesized silver nanoparticles using leaf extract of the neem (*Azadirachta indica*) plant. They noted that at temperatures of 30 °C and 40 °C, silver nanoparticles were not successfully produced. When the temperature was increased to the range of 50–70 °C, nanoparticle formation was initiated, with maximum production observed at 70 °C [70]. Nagar and Devra (2018), demonstrated the impact of temperature on the biosynthesis process while deriving copper nanoparticles using *Azadirachta indica* leaf extract [71]. Elia et al. (2014) reported that the eco-friendly synthesis of gold nanoparticles utilizing leaf-derived extracts from Salvia officinalis as well as Lippia citriodora requires a temperature rise to 35–40 °C to reduce the Au (II) ions [72]. Coman et al. (2024) highlighted the role of temperature in the fabrication of platinum nanoparticles using bark-derived extracts from three *Quercus* species. They noticed that the nanoparticles did not form at low temperatures. Only when the temperature was raised to 70 °C did the solution exhibit a color change from light yellow to dark brown, confirming the synthesis of platinum nanoparticles [62]. In 2022, Al Awadh et al. examined the effect of temperature on the production of ZnO nanoparticles using leaf extract of *Raphanus sativus*. They reported that no surface plasmon resonance peak was detected at 60 °C and 70 °C; however, a distinct peak appeared when the temperature was increased to 80 °C and 90 °C. However, the bandgap value obtained at 80 °C was closest to the theoretical value, making it the optimal reaction temperature [66]. According to Hirphaye et al. in 2023, a temperature of 60 °C was optimal for a higher yield of magnesium oxide nanoparticles derived from the flower extract of *Hagenia abyssinica*. They observed a reduced yield of nanoparticles when the temperature was either increased above 60 °C or decreased below 60 °C [67].

4.3. Contact Time

Several studies have highlighted the crucial role of contact time in nanoparticle synthesis. Rajput et al. (2020) assessed the effect of reaction duration on the synthesis of silver nanoparticles using leaf extract of *Atropa acuminata*. The absorbance was measured at various time intervals (30, 60, 120, and 180 min). An SPR peak was observed at 424 nm after 30 min, confirming the formation of silver-based nanomaterials. After allowing the mixture to stand for 180 min and subsequent analysis, no change in the SPR peak was observed, indicating that 30 min was sufficient for the complete reduction of the silver salt [58]. A similar observation was reported by Verma and Mehta (2016) [73]. Das et al. (2019) reported findings that contradicted those of Rajput et al. According to their study, the complete synthesis of silver nanoparticles required a total incubation time of 2 h during biosynthesis using Atropa belladonna extract [74]. Riyanto et al. (2022) documented the role of storage time in the synthesis of EO-AgNPs derived from the essential oil of *Cymbopogon citratus*. The effect of storage time can be visually observed by a brownish color change. Additionally, the characteristic peak observed at 430 nm after 24 h disappeared after 9–11 days of storage [75]. Saif et al. (2016) evaluated the size of copper oxide nanostructures and observed that the particle size increased to 634.4 ± 40.2 nm after a 72h incubation period, compared to an initial size of 212.6 ± 47.26 nm [76]. In a study by Hirphaye et al., increasing the incubation time from 30 min to 120 min during the formation of magnesium oxide nanostructures from a flower infusion of *Hagenia abyssinica* resulted in the highest absorbance. However, the absorbance decreased when the incubation time was further extended beyond 120 min up to 240 min. Additionally, an increase in nanoparticle size was observed, leading the authors to conclude that 120 min was the optimal incubation time for obtaining smaller nanoparticles [67].

4.4. Metal Salt Concentration

Many studies have reported that the type and concentration of metal salts are directly associated with the hue of the reaction mixture and the structure of the resulting nanoparticles [77]. Rajput et al. (2020) found that increasing the concentration of $AgNO_3$ enhanced the synthesis of silver nanoparticles up to 5 mM; however, beyond this concentration, a distorted peak was observed [58]. Saini et al. (2019) also reported similar findings, observing that the production of silver nanoparticles increased with an increase in $AgNO_3$ concentration [78]. Riyanto et al. (2022) evaluated the influence of $AgNO_3$ concentration on the synthesis of EO-AgNPs by conducting experiments at varying concentrations of 2, 4, 6, 8, and 10 mM. It was observed that nanoparticles synthesized using 2 mM $AgNO_3$ exhibited a lighter color, whereas those synthesized using 10 mM $AgNO_3$ appeared significantly darker. The absorbances at AgNO3 concentrations of 2, 4, 6, 8, and 10 mM were 0.392, 0.472, 0.543, 0.573, and 0.663, respectively. Upon UV–Vis spectrophotometric analysis, the nanoparticles formed at 6, 8, and 10 mM $AgNO_3$ were found to be more stable [75]. As reported by Nagar and Devra, an increase in the size of copper nanoparticles from 48.01 to 78.51 nm when the concentration of copper chloride was increased from 6×10^{-3} M to 7.5×10^{-3} M. They suggested that a higher concentration of copper chloride leads to the formation of a greater number of nuclei [71].

Coman et al. (2024) carried out the synthesis of platinum nanoparticles using different concentrations of K_2PtCl_6, specifically 0.1 mM, 1 mM, and 5 mM. The authors concluded that while a 5 mM concentration of K_2PtCl_6 solution inhibited the synthesis of nanoparticles altogether, a lower concentration of 1 mM resulted in the most efficient reaction, making 1 mM concentration of K_2PtCl_6 the optimal concentration [64]. In a study conducted by Nadeem et al. (2024), the concentration of the precursor salt was found to influence the shape and size of the synthesized nanoparticles. The authors stated that the copper oxide nanoparticles synthesized from 0.25 M copper (II) acetate [$Cu(OAc)_2$] had an approximate size of 34 nm and exhibited interlinking voids and pores. Upon increasing the metal salt concentration to 0.5 M, the nanoparticle size increased to 44 nm, while maintaining a spherical to irregular planar morphology. Similarly, the magnesium oxide nanoparticles synthesized from 0.25 M magnesium sulfate ($MgSO_4$) had an average size of 30 nm. Upon increasing the concentration to 0.5 M, the average nanoparticle size increased to 38 nm. Iron oxide nanoparticles synthesized from 0.25 M ferric chloride ($FeCl_3$) were observed to be cylindrical with an average size of 53 nm, whereas those synthesized from 0.5 M $FeCl_3$ exhibited a spherical morphology with a mean size of 31 nm. Additionally, the activities of magnesium oxide and iron oxide nanoparticles were lower at 0.5 M compared to those synthesized at 0.25 M metal salt concentration [79]. In 2023, Hirphaye et al. highlighted the role of precursor concentration in the biosynthesis of nanoparticles. During their experiment on the synthesis of magnesium oxide nanoparticles using flower extract of *Hagenia abyssinica* and magnesium nitrate hexahydrate as the precursor, they reported that increasing the precursor salt concentration from 0.5 mM to 1 mM resulted in higher absorbance and improved nanoparticle yield. However, any further increase in concentration led to a decrease in absorbance, thereby establishing precursor concentration as an important parameter in the green synthesis of nanoparticles [67].

5. An Overview of the Different Types of Plant-Derived NPs

5.1. Metal-Based Nanoparticles

Nanoparticles can be categorized as organic, inorganic, and carbon-based types based on their chemical nature and structural characteristics. Organic nanoparticles include micelles, liposomes, and dendrimers, whereas inorganic nanoparticles, which lack carbon, include metal nanoparticles composed of pure metals [80]. Figure 4 illustrates this classification. Metal nanoparticles have recently gained significant attention due to their wide range of applications, spanning pharmaceutical fields to various cosmetic products used in daily life [81]. Metallic nanoparticles can be generated in large-scale industries by employing a downstream process optimization. Various metallic nanoparticles are derived from different metals, including silver, gold, platinum, palladium, zinc, copper, titanium, magnesium, and others. The unique properties of metallic nanoparticles, such as distinctive optical characteristics, high stability, and quantum size effects, enable their application across diverse fields, including the food industry, agriculture and crop production, cosmetics, the pharmaceutical sector, and wastewater treatment. Based on the number of metals in their composition, they are categorized as monometallic, bimetallic, trimetallic, and polymetallic nanoparticles. As their names suggest, monometallic nanoparticles are composed of a single metal, bimetallic nanoparticles consist of two metals, trimetallic nanoparticles contain three metals, and polymetallic nanoparticles comprise more than three met-

2026, Vol. 2, Article ID. 2026.0024
https://doi.org/10.69709/SusProc.2026.171930

als [46]. An overview of selected studies on plant-mediated synthesis of metal-based nanoparticles, along with their key characteristics and applications, is presented in Supplementary Table S3 [58,75,82–105].

5.1.1. Monometallic Nanoparticles

The synthesis of monometallic nanoparticles has garnered significant interest in recent years due to their ease of preparation and wide range of applications across various fields. Monometallic nanoparticles can be further categorized into metallic, transition, and magnetic nanoparticles on the basis of the type of metals present in them. The synthesis of silver and gold nanoparticles is widely recognized as the most prevalent choice among researchers [46]. Various monometallic nanoparticles prepared in recent years using metals such as platinum, silver, copper, palladium, and gold are described below:

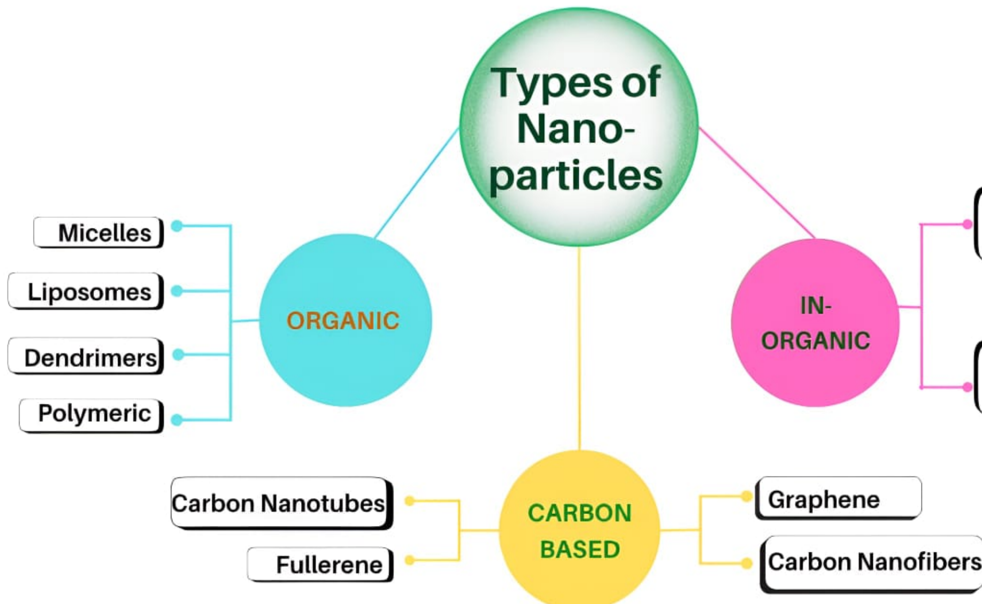

Figure 4: Classification of nanoparticles based on their composition into organic, inorganic, and carbon-based categories. Organic nanoparticles include micelles, liposomes, dendrimers, and polymeric forms; inorganic nanoparticles comprise metal and metal-oxide nanomaterials; while carbon-based nanoparticles include fullerenes, carbon nanotubes, graphene, and carbon nanofibers. This classification highlights the structural diversity and broad functional applications of nanomaterials across biological and industrial fields.

5.1.1.1. Silver Nanoparticles

In ancient times, various forms of silver were used as food preservatives, and the use of silver utensils was common due to their antimicrobial properties. Silver nanoparticles have attracted significant attention over the past one to two decades due to their pronounced cytotoxic activity against various pathogenic microorganisms, including bacteria, protozoa, and fungi [106]. The unique characteristics of silver nanoparticles include high catalytic and antimicrobial activity, high electrical and thermal conductivity, and chemical stability [107]. According to Larue et al. (2014), silver nanoparticles were among the most widely produced nanoparticles globally, with an estimated annual production of approximately 500 tons [108]. Numerous researchers have successfully synthesized silver nanoparticles using a wide range of plant components—including leaves, fruits, stems, roots, flowers, and bark—owing to the presence of diverse phytochemicals within these materials. Khosravi et al. (2023) demonstrated that silver nanoparticles synthesized by the green route using *Malva sylvestris* extract effectively suppressed egg hatching and enhanced juvenile mortality of the root-knot nematode *Meloidogyne javanica* under both laboratory and greenhouse conditions, highlighting their promise as an environmentally friendly nematicidal agent [109]. Onitsuka et al. (2019) reported the synthesis of silver nanoparticles using black and green tea infusions prepared from the leaves of *Camellia sinensis*. Transmission electron microscopy (TEM) analysis revealed that nanoparticles synthesized using green tea extracts had an average size of 18.9 ± 4.4 nm, whereas those produced using black tea extracts exhibited a larger average particle size of 34.4 ± 9.6 nm. The nanoparticles exhibited a spherical morphology and were relatively stable. The nanoparticle colloidal solution was used to dye cotton fabrics, providing antimicrobial activity against *K. pneumoniae* and *S. aureus* [110].

Findings from recent work utilizing *Hyoscyamus muticus* L. extract for the green synthesis of silver nanoparticles demonstrated strong nematicidal activity against *Meloidogyne javanica* while maintaining biocompatibility with host plants. The biogenic AgNPs effectively reduced egg hatching and juvenile survival rates, thereby enhancing the plant's natural defense mechanisms without exhibiting any observable phytotoxic effects. These results emphasize that green-synthesized nanoparticles, owing to their eco-friendly origin and low toxicity, hold considerable promise as replacements for hazardous synthetic agents [111]. In another study, leaves of *Solanum nigrum* were used to synthesize silver nanoparticles by stirring the *Solanum nigrum* leaf extract with silver nitrate for 10 min, as reported by Vigilvani et al. (2019). Spherical, small-sized silver nanoparticles were obtained (1.74–6.96 nm), exhibiting pronounced antimicrobial and catalytic activity [112]. Silver nanoparticles with an average size of 30 nm were synthesized using a leaf-derived solution of Ligustrum lucidum. As reported by Huang et al. (2020), these nanoparticles exhibited antifungal activity against Setosphaeria turcica, with a half-maximal inhibitory concentration (IC50) of 170.20 μg/mL. Moreover, the silver nanoparticles exhibited enhanced antifungal activity when combined with epoxiconazole in 9:1 and 8:2 ratios [113].

Bekhradian et al. (2024) demonstrated the potential of *Malva sylvestris* extract as a biogenic reducing and stabilizing agent for the synthesis of silver and silver oxide nanostructures. The phytochemical components of the extract, including phenolics and flavonoids, play a crucial role in reducing Ag^+ ions and stabilizing (capping) the resulting nanoparticles. These biosynthesized Ag/Ag_2O nanostructures exhibited notable antimicrobial and antioxidant activities, confirming the synergistic effect of the plant-derived biomolecules and the metallic core [114]. Qais et al. (2020) demonstrated the synthesis of silver nanoparticles using seed extract of *Carum copticum* under constant stirring at ambient temperature. The resulting nanostructures predominantly exhibited a spheroidal morphology with varying sizes and demonstrated antivirulence and antibiofilm properties [115]. The production of silver nanoparticles was also documented by Odeniyi et al. (2019), using aqueous and methanolic fruit extracts of *Nauclea latifolia*. The particles were irregularly shaped with an average size of 10 nm, as analyzed by SEM. The resulting nanoparticles exhibited a broad range of applications; however, those synthesized using aqueous fruit extract were found to be more efficient than those prepared using methanolic fruit extract. They showed antibacterial properties against most of the pathogens they were tested for (*C. Freundii, Staphylococcus* sp., *S. aureus, Escherichia coli*, and *Klebsiella* sp.), antifungal properties (*Rhizopus* sp. and *Candida albicans*). The nanoparticles were also used to formulate cold creams, which were found to be aesthetically appealing and satisfactory, and they demonstrated antimicrobial and antifungal activity against several tested pathogens [116]. According to Rajabi et al. (2016), plant extracts such as those from *Suaeda Acuminata* provide bioreductants and stabilizing compounds, enabling green synthesis of silver nanostructures without surfactants or templates, thereby lowering cost and complexity [117].

5.1.1.2. Gold Nanoparticles

Gold has long been regarded as a symbol of wealth and prosperity. Its use in jewelry, ornaments, royal palaces, and crowns is well documented throughout history. In India, gold ash was also used as an Ayurvedic medicine in ancient times. Although bulk gold is largely inert, it exhibits unique properties at the nanoscale. Gold nanoparticles have attracted significant attention over the past few decades despite their relatively high cost, owing to their wide range of industrial applications. These include minimal to no toxicity toward human cells, good solubility and stability, catalytic activity, ease of one-step green synthesis, ability to conjugate with proteins, as well as applications in disease diagnostics, gene expression studies, and drug delivery [46]. Elia et al. (2014) reported the fabrication of gold nanoparticles using fruit extract of *Punica granatum* and leaf extracts of *Pelargonium graveolens*, *Lippia citriodora*, and *Salvia officinalis*. The nanoparticles demonstrated excellent biocompatibility and stability [72]. According to Patil et al. (2023), fruit extract of *Capsicum annuum* can be used in the production of gold nanoparticles. This synthesis was carried out at 90 °C with vigorous stirring for several minutes. The transition in mixture color from pale yellow to deep violet signified the formation of gold nanoparticles. The obtained nanoparticles exhibited a spherical shape, with sizes ranging from 20 to 30 nm and an average diameter of 25.92 nm. The nanoparticles exhibited dose-dependent antioxidant activity against DPPH (86.0% at 100 μg/mL), anti-inflammatory activity (IC50 = 619.4 μg/mL) within a concentration range of 100–1200 μg/mL, and anti-angiogenic effects at 100 μg/mL [118].

Fouda et al. (2022) synthesized gold nanoparticles with crystalline, spherical morphology using an $HAuCl_4$ solution and an aqueous extract of *Zingiber officinale* rhizome. The nanoparticles exhibited a size distribution ranging from 5 to 53 nm, with an average size of 15.11 ± 8.5

nm. The synthesis was carried out at pH 8 and 60 °C for 60 min. The effective synthesis of gold nanoparticles was indicated by a color shift in the solution from pale yellow to purple. The synthesized nanoparticles showed dose-dependent antimicrobial activity towards *Bacillus subtilis, Escherichia coli, Aspergillus brasiliensis, Pseudomonas aeruginosa, Staphylococcus aureus, Candida albicans*, and *Pseudomonas aeruginosa*, with the highest zone of inhibition, ZOI, at a concentration of 200 μg/mL. The antioxidant activity of the gold nanoparticles against DPPH was expressed as an IC_{50} value of approximately 16 μg/mL, indicating a slightly lower effect compared with ascorbic acid, which served as the standard and showed an IC_{50} value of 12.8 μg/mL. Additionally, the cytotoxic effects of the gold nanoparticles on adenocarcinoma (MCF-7) and hepatocellular carcinoma (HepG2) cell lines were recorded with IC_{50} values of 288.23 ± 31.39 μg/mL and 131.9 ± 9.34 μg/mL, respectively, while showing negligible toxicity toward normal oral epithelial cells (IC_{50} = 487.612 ± 3.53 μg/mL) [119]. In another work by Ahmad et al. (2024) reported the synthesis of gold nanoparticles using crude extract of *Aconitum violaceum* under constant stirring at pH 9 for 50 min. Following SEM and TEM analysis, the particles exhibited spherical morphology with sizes below 100 nm, as well as triangular morphology with sizes approaching 100 nm. The nanoparticles showed potent antibacterial, antioxidant, and photocatalytic activity [120].

5.1.1.3. Copper Nanoparticles

Copper has long been used in medical and dental fields due to its antimicrobial, anti-inflammatory, and low-toxicity properties [121]. In the literature, extensive data are available on the plant-mediated biosynthesis of copper nanoparticles and their wide-ranging applications. Copper nanoparticles are obtained by reducing Cu^{2+} ions from a copper salt solution to the Cu^0 form. Bioactive compounds present in plant extracts contribute to the stability of the nanoparticles [122]. The size and morphology of copper nanostructures are largely influenced by the concentration of the precursor salt, as demonstrated by Nagar and Devra (2018) during the synthesis of copper nanoparticles using leaf extracts of *Azadirachta indica* [71]. Mehdizadeh et al. (2020) reported the synthesis of copper nanoparticles using cellulosic walnut shell as a base material. The process was initially carried out at 50 °C for a duration of 2 h. In the subsequent step, the reduction of Cu^{2+} ions was achieved by adding an ethanol solution of NaBH4 and stirring for another 3 h. The nanoparticles were found to be thermally stable up to 200 °C. TEM analysis revealed three distinct types of nanoparticles: CuNPs with sizes ranging from 15–22 nm, CuNPs with sizes ranging from 60–80 nm, and unsupported CuNPs. The nanoparticles exhibited antimicrobial properties against *Escherichia coli, Listeria monocytogenes*, and *Staphylococcus aureus*, antioxidant properties for DPPH, and cytotoxic properties for K562 (erythroleukemia) cell line with an IC_{50} value of 25.24 ± 5 μg/mL in a dose-dependent manner [123].

Mali et al. (2020) synthesized spherical copper nanoparticles from a $CuSO_4 \cdot 5H_2O$ solution and an aqueous leaf extract of *Celastrus paniculatus*. The reaction pH was adjusted to 7.0. The obtained particles were 2–10 nm in size, with a mean diameter of 5 nm. The nanoparticles exhibited good photocatalytic properties and antifungal activity against *Fusarium oxysporum*. At copper nanoparticle concentrations of 0.24%, 0.18%, and 0.12%, mycelial growth inhibition was recorded as 76.29 ± 1.52%, 73.70 ± 1.52%, and 59.25 ± 0.57%, respectively [124]. According to Amjad et al. in 2021, the copper nanoparticles can be synthesized from the leaf extract of *Fortunella margarita* and $CuSO_4.5H_2O$ solution at 70 °C and 5.5 pH for 30 min. The color change from dark green to bluish green indicated the successful formation of nanoparticles. The nanoparticles appeared spherical but were agglomerated, exhibiting sizes ranging from 51.26 to 56.66 nm under SEM analysis [63]. Sharma et al. (2018) synthesized copper nanoparticles using leaf extracts of *Tinospora cordifolia* and a $CuCl_2$ solution at 85 °C for 20 min. The particles exhibited a spherical morphology with sizes ranging from 50 to 130 nm. The synthesized nanoparticles showed excellent catalytic degradation towards reactive dye, eosin yellowish, safranin, and direct dye [125]. Mali et al. (2020) utilized secondary metabolites from leaf extract of *Celastrus paniculatus* to synthesize copper nanoparticles. SEM and TEM images revealed that the particles exhibited a spherical morphology with a size range of 2–10 nm. Plant-synthesized copper nanoparticles demonstrate effective catalytic degradation of methylene blue (MB) and notable antifungal activity against *Fusarium oxysporum*, exhibiting 76.29 ± 1.52% mycelial growth inhibition at a concentration of 0.24% copper nanoparticles [124].

5.1.1.4. Palladium Nanoparticles

Palladium nanoparticles have a broad applicability in bioscience, biomedicine, and pharmacy. These nanoparticles have attracted considerable attention due to their high surface-area-to-volume ratio, which enables them to function as highly efficient and selective catalysts, depending on their morphology, as reported by Cheong et al. [96]. A variety of plant-derived phytochemicals facilitate the green synthesis of palladium nanoparticles by reducing Pd (II) ions present in palladium salts [1]. Petla et al. synthesized palladium nanoparticles using leaf extracts of *Glycine max*. The leaf extract contains various polyols, terpenoids, and reducing sugars, which act as reducing agents for the synthesis of palladium nanoparticles. The resulting nanoparticles exhibited a face-centered cubic (FCC) crystalline structure with a size of 15 nm [96]. Vinodhini et al. (2022) reported the plant-mediated synthesis of palladium nanoparticles using leaf extracts of *Allium fistulosum*, *Basella alba*, and *Tabernaemontana divaricata*, with particle sizes of 500 nm, 2 μm, and 2 μm, respectively. The obtained nanoparticles exhibited a spherical morphology. Nanoparticle formation was indicated by a color change from mild brown to dark brown in *T. divaricata* and A. fistulosum, while a transition from pale brown to green was observed in the case of *Basella alba*. The nanoparticles were further evaluated for their biomedical application. They exhibited highly effective antibacterial activity against *Bacillus cereus, Bacillus subtilis, Escherichia coli*, and *Staphylococcus aureus*, with the highest antibacterial effect observed at a concentration of 100 μL. They also demonstrated antifungal activity against *Aspergillus flavus, Penicillium* sp., and *Candida albicans*, with particle sizes of 150, 100, and 50 nm, respectively. Palladium nanoparticles synthesized from *Basella alba* also exhibited the highest antioxidant activity at 1000 μg concentration as compared to others. The nanoparticles also showed dose-dependent anti-diabetic properties by repressing alpha-amylase enzyme.

Additionally, the nanoparticles exhibited good photocatalytic activity [99]. Sattar et al. (2024) utilized root extract of *Curcuma longa* for the biosynthesis of palladium nanoparticles. The reaction mixture was continuously stirred at 70 °C for 3 h. The generated nanoparticles were characterized as spherical, with sizes ranging from 50 to 150 nm. Palladium nanoparticles showed dose-dependent antioxidant activity, antifungal activity towards *Candida* sp., with the highest zone of inhibition reported as 17 ± 0.28 mm at 130 μg/mL. Similar results were observed when evaluating their antibacterial efficiency against *Staphylococcus aureus* and *Escherichia coli*, with maximum inhibition zones of 17 ± 0.28 mm and 27 ± 0.22 mm, respectively, at a concentration of 130 μg/mL. The palladium nanoparticles also inhibited the MCF-7 breast cancer cell line in a concentration-dependent manner, with the highest inhibition observed at 130 μg/mL (26.53% ± 2.45) compared with untreated control cells [126]. Bathula et al. (2020) used leaf extracts of *Coleus amboinicus* to derive palladium nanoparticles ultrasonically. The transformation of the precursor solution from brown to black indicated the successful formation of palladium nanoparticles. Further analysis using HRTEM and TEM confirmed that the nanoparticles possessed a spherical, crystalline structure with sizes ranging from 16 to 23 nm and an average diameter of 20 nm. The palladium nanoparticles were found to serve as highly efficient catalysts in ultrasound-assisted Suzuki–Miyaura coupling reactions [127].

5.1.1.5. Platinum Nanoparticles

Platinum nanoparticles have been extensively studied, particularly for their applications in the biomedical field. Patel et al. investigated the potential of platinum nanoparticles in nanomedicine and for their antibacterial properties [128]. In another study, Sahin et al. (2016) investigated *Punica granatum*-mediated platinum nanoparticles and evaluated their cytotoxic effects against the human breast cancer cell line MCF-7 using the MTT assay. Platinum nanoparticles showed a dose-dependent inhibition in the proliferation of MCF7 cells by inducing cell apoptosis during the G0/G1 phase [129]. Zhang et al. (2022) performed the green synthesis of platinum nanoparticles utilizing the floral extract of *Nymphaea tetragona*, in the H_2PtCl_6/*N.tetragona* floral extract ratio of 1:4 and 1:1, and confirmed the average particle size of formed nanoparticles as 2.01 ± 0.80 nm and 4.04 ± 1.31 nm, respectively. The authors evaluated the use of platinum nanoparticles in anti-aging and skin lightening. Upon culturing the human melanogenic cell line (A375) with platinum nanoparticles, it was revealed that both types of nanoparticles exhibit dose-dependent inhibition of melanin production by inhibiting the tyrosinase enzyme. They also inhibited UVB-induced melanin synthesis. In studies on the human skin fibroblast cell line (HFF-1), the nanoparticles were confirmed to exhibit anti-aging activity by enhancing collagen I production through activation of the underlying molecular mechanisms, including the TGF-β and Smad signaling pathways responsible for collagen I synthesis [105]. In another study, Eltaweil et al. (2021) prepared platinum nanoparticles using leaf extracts of *Atriplex halimus*. The reaction was carried out at pH 9.6 and 95 °C under constant stirring for approximately one hour, after which a color change from dark yellow to black was observed. The prepared nanoparticles exhibited particle sizes ranging from 1 to 3 nm and predominantly displayed a spherical morphology. The nanoparticles exhibited excellent catalytic, antioxidant, and antibacterial activity [100]. In a similar study conducted by Coman et al. (2024), platinum nanoparticles were synthesized using bark extracts of *Quercus petraea*, *Quercus frainetto*, and *Quercus dalechampii*, yielding nanoparticles with average diameters of 41 ± 5.3 nm, 41.6 ± 4.4 nm, and

58.5 ± 7.6 nm, respectively. The synthesized nanoparticles had a spherical morphology and showed superb antioxidant properties, with Nanoparticles synthesized from *Q. petraea* having the maximum DPPH (539 mg GAE/g dw), FRAP (783 mg GAE/g dw), and CUPRAC (573 mg GAE/g dw) free radical scavenging activity, while nanoparticles synthesized from *Q. dalechampii* showed the highest ABTS free radical scavenging activity (605 mg GAE/g dw). The nanoparticles also exhibited potent antimicrobial activity against certain bacteria and fungi, particularly *Escherichia coli, Enterococcus faecalis, Candida krusei*, and *Candida auris* [64].

5.1.2. Bimetallic Nanoparticles

The bimetallic nanoparticles resulted because of the discovery of hybrid nanoparticle synthesis in which two distinct metals are combined in a reaction vessel under carefully controlled conditions [130]. They can be classified into two types: (i) those in which both metals are homogeneously mixed within the same particle, and (ii) core–shell structures, in which one metal forms a core that is encapsulated by another metal forming the shell. Figure 5 illustrates the green synthesis of Ag–Cu bimetallic nanoparticles using *Salvia officinalis* leaf extract, where phytochemicals act as reducing and capping agents during nanoparticle formation [131]. These nanoparticles are considered particularly significant as they overcome the limitations of their corresponding monometallic counterparts and enhance their overall properties [46]. Bimetallic nanoparticles exhibit distinct physical properties, including high surface area, quantum effects, enhanced mobility, and improved thermal, catalytic, magnetic, mechanical, chemical, and optical characteristics, making them superior to their monometallic counterparts [130]. As reported by Fahmy et al. (2021), platinum–palladium (Pt–Pd) bimetallic nanoparticles synthesized using seed extract of *Peganum harmala* at 60 °C for 24 h were more functionally efficient than their individual platinum and palladium counterparts. In the FRAP assay, platinum–palladium nanoparticles (843 ± 60 μM TE/mg) exhibited approximately four times higher antioxidant activity than the harmala alkaloid fraction (33.91 ± 5.82 μM TE/mg), as well as greater activity than platinum nanoparticles (277.3 ± 13.5 μM TE/mg) and palladium nanoparticles (167.6 ± 4.8 μM TE/mg). Upon evaluation of their cytotoxic activity against human breast cancer (MCF-7) and lung cancer (A549) cell lines, it was observed that platinum–palladium nanoparticles exhibited significantly higher cytotoxicity, with IC_{50} values of 3.6 and 8.8 μg/mL, respectively. In comparison, platinum nanoparticles showed IC_{50} values of 6.7 and 10.9 μg/mL, while palladium nanoparticles demonstrated comparatively lower cytotoxic effects, with IC_{50} values of 10.8 and 31 μg/mL, respectively [84].

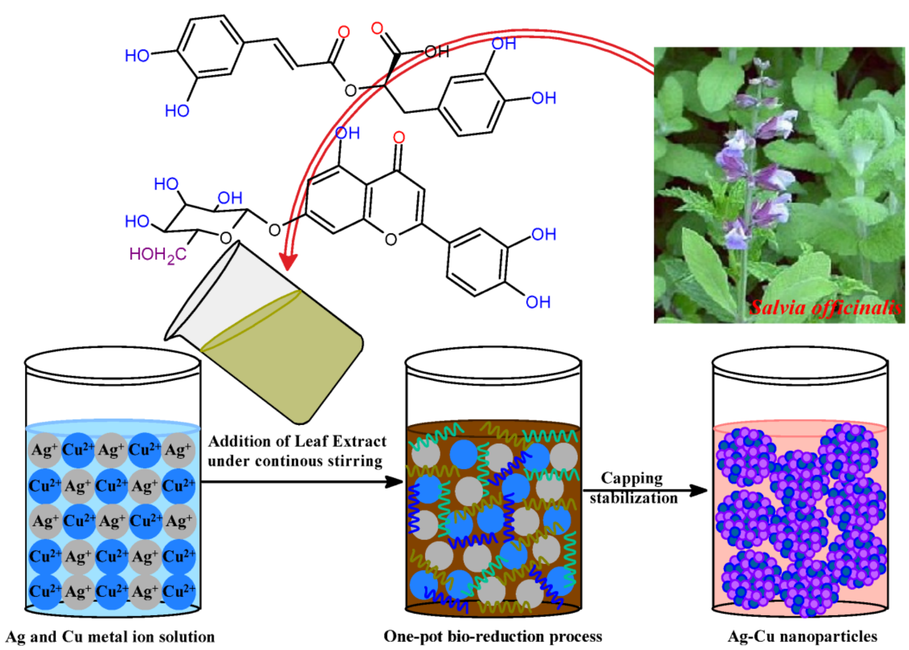

Figure 5: Schematic representation of the green synthesis of Ag–Cu bimetallic nanoparticles using *Salvia officinalis* leaf extract. The bio-reduction and capping processes are mediated by phytochemicals, such as polyphenols and flavonoids, present in the extract, thereby stabilizing Ag–Cu nanoparticles. (Adapted from Malik et al., 2023 [131] under the license by CCBY 4.0).

A study by Ashishie et al. (2018) documented the eco-friendly synthesis of Ag–Cu bimetallic nanoparticles using an aqueous infusion of *Kigelia africana* fruits under reflux at 120 °C for 6 h. The resulting nanoparticles were crystalline in nature, with an average size of 10 nm, and demonstrated greater effectiveness against both Gram-positive and Gram-negative bacteria compared with the antibiotics tested, including Augmentin, Meropenem, Ofloxacin, Ciprofloxacin, and Racinef [132]. *Moringa oleifera* leaf extract was used to synthesize Ni/Fe_3O_4 MNPs at 70 °C by Prasad et al., 2017. The nanoparticles exhibited a spherical morphology, with diameters ranging from 16 to 20 nm. Ni/Fe_3O_4 nanoparticles functioned as a magnet adsorbent for the removal of Malachite green dye from an aqueous solution [133]. Luo et al. (2016) also documented the fabrication of Fe/Pd bimetallic nanoparticles using an aqueous extract of grape leaves. The process was carried out at ambient temperature for 30 min. The synthesized nanoparticles exhibited a spherical shape with sizes ranging from 20–100 nm [134]. A study by Mamatha et al. (2020) reported the fabrication of Ag-Cu nanoparticles on cotton fabrics utilizing aloe vera leaf extract by constant stirring for 24 h. These nanoparticle-incorporated cotton fabrics were used in medical applications, particularly as wound dressings [135].

5.1.3. Trimetallic Nanoparticles

Trimetallic nanoparticles are synthesized by combining three different metals or metal oxides. They typically exhibit a "triple core–shell architecture," in which one element forms the core, a second element constitutes an intermediate layer surrounding the core, and a third element forms the outer shell [136]. Figure 6 illustrates the eco-friendly synthesis of Cu–Co–Ni trimetallic nanoparticles using *Origanum vulgare* extract, emphasizing the bio-reduction and stabilization processes mediated by plant-derived phytochemicals [137]. Polymetallic or trimetallic nanoparticles have attracted significant attention for many years due to their enhanced biological properties compared with single-metal and bimetallic nanoparticles [138]. Compared with mono- or bimetallic nanoparticles, they exhibit enhanced stability, greater morphological diversity, and improved catalytic and antibacterial properties, as well as other therapeutic activities [139]. Their optical, magnetic, electronic, and catalytic properties arise from the synergistic effects of the constituent metals, thereby broadening their applications to catalysis, antimicrobial and antibiofilm activity, biomedicine, and sensing. Trimetallic nanoparticles have also been incorporated into food packaging, as reported in several studies [140]. To date, plant-mediated fabrication of trimetallic nanoparticles has been scarcely explored, as highlighted in the literature. A recent study by Farooq et al. (2025) highlighted the effectiveness of green-synthesized Co–Fe–ZnS nanocomposites prepared using plant extract of *Avena fatua*. The nanocomposites demonstrated remarkable multifunctional activity, including photocatalytic degradation of amoxicillin, hydrogen generation, and CO_2 reduction. The study further optimized reaction conditions through response surface methodology (RSM), confirming the material's potential for sustainable and scalable photocatalytic applications. Such findings emphasize how combining multiple metal ions within a single nanosystem can significantly improve photocatalytic performance while adhering to environmentally friendly synthesis principles [141].

Vaseghi et al. (2018) synthesized Cu–Cr–Ni oxide trimetallic nanoparticles using aqueous leaf infusions of *Eryngium campestre* and *Froriepia subpinnata* as both reducing and capping agents. The process was carried out for 3 min at 34 °C with the addition of precursor salts ($Cr(NO_3)_3 \cdot 9H_2O$, $Ni(NO_3)_2 \cdot 6H_2O$, and $CuSO_4 \cdot 5H_2O$) along with *E. campestre* leaf extract, while for *F. subpinnata* leaf extract, the temperature was maintained at 40 °C. The transformation from transparent brown to colloidal brown confirmed the synthesis of trimetallic oxide nanoparticles. FESEM analysis revealed that the nanoparticles exhibited a nanoplates morphology, with average thicknesses of 14.15 nm, 10.96 nm, and 18.73 nm for the mixed leaf extract, *F. subpinnata*, and *E. campestre*, respectively. The nanoparticles exhibited strong antibacterial properties against *Staphylococcus aureus* and *Escherichia coli* [142].

Kannaiyan et al. (2021) documented the fabrication of trimetallic oxide Ni–Cr–Cu nanoparticles using leaf extract of *Coriandrum sativum*. $Cr(NO_3)_3 \cdot 9H_2O$, $Ni(NO_3)_2 \cdot 6H_2O$, and $CuSO_4 \cdot 5H_2O$ were used as precursor salts. The process was carried out for 45 min in a water bath maintained at 40 °C. The synthesized nanoparticles exhibited dose-dependent antibacterial and antifungal activity, with the highest zone of inhibition (ZOI) observed at 1000 µg/mL, measuring 27 mm, 24 mm, 23 mm, and 15 mm against *E. coli*, *Staphylococcus aureus*, *A. flavus*, and *Penicillium* sp., respectively [143].

In a similar study, Hussein et al. (2022) investigated the fabrication of Ru/Ag/Pd nanoparticles using an aqueous extract of garlic tunicate leaves. The obtained nanoparticles exhibited a spherical morphology, with sizes ranging from 50 to 90 nm. The nanoparticles exhibited significant antimicrobial activity against all tested microorganisms, including *B. cereus*, *A. niger*, *C. glabrata*, *A. flavus*, *E. coli*, and *C. albicans*. Notably,

2026, Vol. 2, Article ID. 2026.0024
https://doi.org/10.69709/SusProc.2026.171930

their efficacy was higher than that of individual palladium, silver, and ruthenium nanoparticles. The nanoparticles also exhibited cytotoxic activity against K562, HepG2, and Caco-2 cell lines, with IC_{50} values of 35.87 ± 2.0, 68.8 ± 3.9, and 47.35 ± 2.7 µg/mL, respectively. These values were further enhanced upon UV exposure, decreasing to 28.32 ± 1.6, 46.77 ± 2.6, and 9.32 ± 0.52 µg/mL, respectively [144]. Radhakrishnan and Subramaniam prepared Cu-Ag-Ru trimetallic nanoparticles using *Andographis paniculata* leaf extract. The reaction was carried out at 70 °C for 1 h, using 0.1 N copper sulfate, silver nitrate, and ruthenium chloride as precursor solutions. The TEM image showed that the synthesized nanoparticles were spherical, exhibited an agglomerated structure, and had a mean size of 22 nm. The nanoparticles exhibited exceptional photocatalytic activity and strong antibacterial activity against E. coli, S. pyogenes, S. aureus, and K. pneumoniae, with the largest zone of inhibition observed at 75 µL. They also demonstrated anticancer activity against human breast cancer cell lines, as well as notable antioxidant properties [145]. Mohammed and Idrees (2024) reported the synthesis of Co–Zn–Ni trimetallic oxide nanoparticles using leaf extracts of *Cicer arietinum*. The resulting nanoparticles exhibited a spherical morphology with an average diameter of 25.72 nm. Furthermore, they demonstrated stronger anti-biofilm activity against *Staphylococcus aureus* compared to the commonly used antibiotic ciprofloxacin [140].

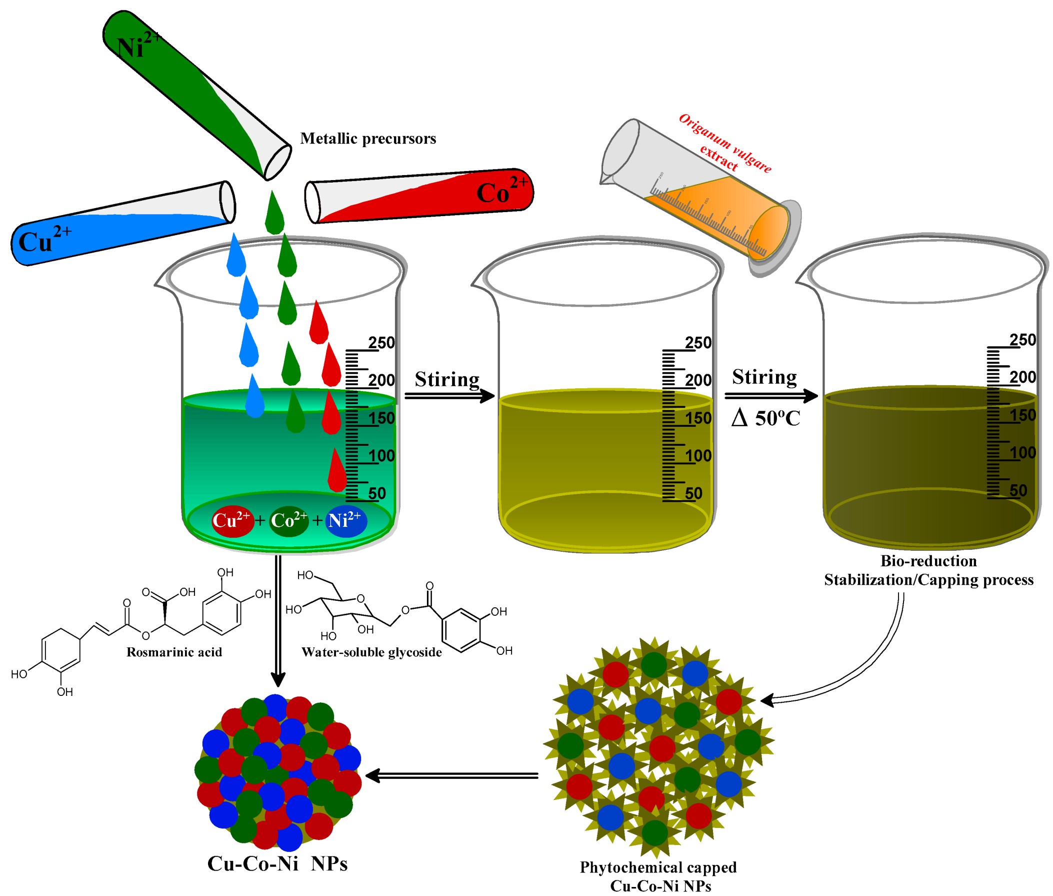

Figure 6: Illustrates the eco-friendly synthesis of Cu–Co–Ni trimetallic nanoparticles using *Origanum vulgare* extract. The phytochemical constituents, including rosmarinic acid and glycosides, act as reducing and stabilizing agents during the bio-reduction and capping process. (Adapted from Alshehri et al., 2020 [137] under the license of CC BY 4.0).

5.2. Metal Oxide-Based Nanoparticles

Metal oxide nanoparticles represent a distinct class of inorganic nanomaterials. A range of metal oxide nanoparticles, including copper oxide, zinc oxide, cerium oxide, cobalt oxide, titanium dioxide, calcium oxide, silicon oxide, manganese oxide, iron oxide nanoparticles, etc., have been cited in scholarly literature. To date, their applications in renewable energy conversion, chemical reactions, sensing systems, data storage technologies, and electronics have been extensively studied [146]. Recent studies have demonstrated the green synthesis of metal oxide nanoparticles, such as γ-Al_2O_3, using plant extracts like *Oxystelma esculentum*, which exhibit excellent photocatalytic efficiency for both pollutant degradation and CO_2 photoreduction. The biogenic approach not only reduces reliance on hazardous chemical precursors but also enhances surface reactivity and stability, thereby highlighting the potential of such nanomaterials for applications in environmental remediation and renewable energy [147]. A similar study by Farooq et al. (2025) investigated the green synthesis of cerium oxide (CeO_2) nanoparticles, highlighting their remarkable photocatalytic activity and potential for environmental remediation. They synthesized CeO_2 nanoparticles using *Ammi visnaga* plant extract and achieved 96.19% degradation of methylene blue within 1 h, along with a CO_2 photoreduction efficiency of 109.27 μmol·g⁻¹·h⁻¹ under optimized conditions [148]. Although plant-mediated fabrication of metal oxide nanoparticles is more complex than that of metal-based nanoparticles, it often requires high-temperature treatment to obtain nanoparticles from metal oxides, as these compounds tend to be less stable. Therefore, to remove oxygen from metal oxides, treatments such as annealing or calcination are employed, typically requiring temperatures above 300 °C [149]. The primary purpose of their synthesis is to enhance the properties of the corresponding metal nanoparticles [80]. Metal oxide nanoparticles exhibit a wide range of unique optical, magnetic, and electrical properties, which has led to their extensive exploration for applications across various fields [146]. Representative studies on plant-mediated synthesis of metal oxide nanoparticles are summarized in Supplementary Table S4 [52,65–67,79,104,150–180].

5.2.1. Copper Oxide Nanoparticles

Due to the magnetic, optical, and electrical properties of copper oxide, there has been accelerated growth in the synthesis of its nanoparticles, which exhibit a broad range of applications. In the existing literature, copper oxide nanoparticles derived from various plants have undergone exploration for their antimicrobial efficacy, photocatalytic activity, and cytotoxic properties [150]. Alhalili Z (2022) reported the fabrication of copper oxide nanoparticles using a leaf extract of *Eucalyptus globulus* as a reducing and stabilizing agent. The synthesized nanoparticles exhibited a spherical morphology with an average diameter of 88 nm. Furthermore, their potential as an adsorbent was evaluated by employing copper oxide nanoparticles for the removal of methyl orange from aqueous environments. Their study indicated a maximum adsorption capacity of 92.2 mg/g under optimized conditions, including an adsorbent dosage of 0.045 g, pH 6, and a temperature of 25 °C [150]. In a study conducted by Nasrollahzadeh et al. (2015), copper oxide nanoparticles were synthesized using flower extracts of *Anthemis nobilis* and subsequently employed as catalysts in the aldehyde–amine–alkyne (A3) coupling reaction [181].

According to Andualem et al. (2020), copper oxide nanoparticles were synthesized using *Catha edulis* extracts, which acted as both stabilizing and reducing agents, with copper nitrate trihydrate serving as the precursor. The reaction mixture was stirred constantly by keeping the temperature at 80 °C until the solution's color shifted from deep green to deep brown. The biosynthesized nanoparticles were observed to exhibit a spherical morphology, as confirmed by SEM and TEM analyses. The authors evaluated the antibacterial activity of the synthesized nanoparticles and reported that those prepared using a leaf extract-to-precursor salt ratio of 1:2 exhibited the highest antibacterial efficacy, with zones of inhibition (ZOI) of 29 $\pm$ 0.03 mm, 32 $\pm$ 0.02 mm, 24 $\pm$ 0.02 mm, and 22 $\pm$ 0.01 mm against *Klebsiella pneumoniae*, *Escherichia coli*, *Streptococcus pyogenes*, and *Staphylococcus aureus*, respectively [182]. Similarly, a study conducted by Abosede et al. (2022) utilized leaf extract from *Justicia carnea* for the synthesis of copper oxide nanoparticles, using copper sulfate pentahydrate as the precursor salt. The formation of a brown precipitate after 40 min confirmed the successful synthesis of nanoparticles [183]. Afzal et al. (2022) documented the synthesis of copper oxide nanoparticles using leaf extracts of *Aerva javanica* and copper sulfate pentahydrate. The process was carried out at pH 11 and maintained at 60 °C for 2 h under constant stirring. The nanoparticles showed an agglomerated structure and had promising potential as antifungal and antibacterial agents [184]. Sukumar et al. (2020) discovered that the seed extract of *Caesalpinia bonducella* can serve as an effective agent for synthesizing copper oxide nanoparticles. The antibacterial potential of the obtained nanoparticles was assessed against *Staphylococcus aureus* and *Aeromonas* [185]. Atri et al. (2023) observed the octahedral crystal clusters of copper oxide nanoparticles synthesized using the aerial parts of *Ephedra alata*. The reaction was carried out at 90 °C for 2 h. The obtained nanoparticles also exhibited photocatalytic activity and antimicrobial potential against *C. albicans* (ZOI = 16.2 mm), *S. cerevisiae* (ZOI = 18.4 mm), *B. Subtilis* (ZOI = 16 mm), and *S. aureus* (ZOI = 20.4 mm). Additionally, biosynthesized copper nanoparticles were found to be much more efficient than chemically synthesized ones [186].

5.2.2. Zinc Oxide Nanoparticles

Zinc oxide, an n-type semiconductor, possesses a high exciton binding energy and a wide band gap, making it suitable for applications in photocatalysis, light-emitting diodes, electrochemical systems, sensors, and solar cells [149]. Plant-extracted Zinc oxide nanoparticles have found widespread applications in the pharmaceutical field owing to their antimicrobial, antilarvicidal, anti-inflammatory, and antitumor properties, as well as their potential in drug delivery and imaging. Their low toxicity and cost-effectiveness have also garnered a considerable amount of attention from the researchers [187]. Manojkumar et al. (2023) reported a hexagonal wurtzite structure for zinc oxide nanoparticles synthesized using leaf extract of *Brassica oleracea* var. *botrytis*, with an average particle size of 52 nm. The nanoparticles displayed good antimicrobial potential against *Escherichia coli* (inhibition zone of 9 mm), *Klebsiella pneumonia* (inhibition zone of 13 mm), *Staphylococcus aureus* (inhibition zone of 13 mm) and *Bacillus subtilis* (inhibition zone of 16 mm) respectively, effective photocatalytic breakdown of methylene blue and larvicidal activity against the larva of *Culex quinquefasciatus* with the LC50 and LC90 value being 76.03 and 190.03 ppm, respectively [188]. Idris et al. (2024) successfully synthesized zinc oxide nanoparticles using leaf extract of *Mariposa christia vespertilioni*. The nanoparticles exhibited an agglomerated and irregular morphology, with particle sizes ranging from 38 to 65 nm. The nanoparticles demonstrated excellent potential as anode materials for sodium-ion batteries (SIBs) [189]. Al-Radadi et al. (2022) synthesized zinc oxide nanoparticles using underground stem extract of *Zingiber officinale*. The reaction was carried out at 60 °C, 11 pH, 60 min of incubation time, and 2.0 mg of metal salt concentration. The authors also revealed that the obtained nanoparticles improved the antibacterial potential of various antibiotics like Ciprofloxacin, Imipenem, Vancomycin, and Amoxicillin-Clavulanic acid against *Escherichia coli* and *Staphylococcus aureus*. The nanoparticles were also found to exhibit hemo-compatible, antioxidant, and anti-inflammatory properties. Additionally, the nanoparticles exhibited anti-diabetic properties by inhibiting alpha-amylase and anti-Alzheimer's properties by inhibiting acetylcholinesterase (AChE) and butyrylcholinesterase (BChE) [91].

Al-Awadh et al. (2022) reported the synthesis of spherical zinc oxide nanoparticles with an average particle size of 66.47 nm using leaf extract of *Raphanus sativus* and zinc acetate dihydrate ($Zn(O_2CCH_3)_2 \cdot (H_2O)_2$) as the precursor salt. The synthesis of nanoparticles was found to be highly efficient at 12 pH and 80 °C and showed good cytotoxicity in inhibiting human breast cancer cells [66]. Karimzadeh et al. (2020) reported the synthesis of spherical ZnO nanoparticles with particle sizes ranging from 20 to 80 nm, using aerial parts of *Acantholimon serotinum* at 60 °C and pH 8 for 6 h. The development of a yellowish-brown coloration indicates the successful formation of nanoparticles. The nanoparticles were further investigated for their anti-cancerous activity against HEK-293 (IC50: 60 μg/mL), MDA-MB-231 (IC50: 24 μg/mL), SH-SY5Y (IC50: 42 μg/mL), and Caco-2 (IC50: 61 μg/mL) [190]. Sana et al. (2020) reported the synthesis of ZnO nanoparticles using leaf extract of *Crotalaria verrucosa*. The biosynthesized nanoparticles exhibited a hexagonal structure with particle sizes ranging from 16 to 38 nm. They also demonstrated promising antimicrobial activity against *Klebsiella pneumoniae*, *Proteus vulgaris*, *Staphylococcus aureus*, and *Escherichia coli*, as well as anticancer potential against DU145 and HeLa cell lines [191].

5.2.3. Iron Oxide Nanoparticles

Iron, one of the most abundant elements in the Earth's crust, has attracted significant interest for the synthesis of nanoparticles. Its oxides exist in four crystalline forms: α-Fe_2O_3, β-Fe_2O_3, γ-Fe_2O_3, and ε-Fe_2O_3. Among these, α-Fe_2O_3, β-Fe_2O_3, and γ-Fe_2O_3 are commonly referred to as hematite, magnetite, and maghemite, respectively. Among these structures, α-Fe_2O_3 (hematite) is the most thermodynamically stable and exhibits desirable properties, including low toxicity, chemical inertness, and biocompatibility. These characteristics have motivated extensive research into its nanoparticle synthesis and its applications across various fields [192]. To date, many methods have been employed to derive α-Fe2O3 nanoparticles, including Sol-gel reactions, co-precipitation, microwave processing, and microemulsion. However, green synthesis is currently being preferred over them. Aida et al. (2023) reported the synthesis of hematite (α-Fe_2O_3) nanoparticles using hibiscus floral extract and $FeCl_3$ solution, resulting in nanoparticles with an average size of 20 nm [193]. Earlier, Miri et al. (2019) described the fabrication of α- Fe_2O_3 nanoparticles using a bark extract of *Salvadora persica*. The reaction was carried out at 70 °C for 2 h, with the pH adjusted to 7 and 11. At pH 7, calcination at 350 °C led to the predominance of maghemite (γ-Fe_2O_3) nanoparticles, whereas calcination at 450 °C favored the formation of hematite (α-Fe_2O_3) nanoparticles. The hematite phase exhibited a spherical morphology with particle sizes ranging from 15 to 20 nm. The study also revealed the superparamagnetic properties of the biosynthesized nanoparticles [161]. Desalegn et al. (2019) reported the synthesis of iron nanoparticles using peel extract of *Mangifera indica* [194].

Rostamizadeh et al. (2020) reported the synthesis of Fe_2O_3 nanoparticles using *Cornus mas* L. fruit extract. The nanoparticles were spherical in morphology, with sizes ranging from 20 to 40 nm. The study indicated the potential of Fe_2O_3 nanoparticles for producing nanofertilizers [195]. Jamzad et al. (2020) also successfully produced Fe_2O_3 nanoparticles using the leaves extract of *Laurus nobilis* L. The nanoparticles exhibited a predominantly spherical morphology with partial hexagonal features, and an average size of 8.03 $\pm$ 8.99 nm. They also demonstrated significant antibacterial and antifungal activity [196]. Buarki et al. (2022) evaluated the antibacterial inhibition efficacy of nearly spherical Fe_2O_3 nanoparticles synthesized using *Hibiscus rosa-sinensis* flower extract and $FeCl_2 \cdot 4H_2O$ in a 2:1 ratio. The nanoparticles were tested against various bacterial strains, including *Escherichia coli*, *Klebsiella pneumoniae*, *Pseudomonas aeruginosa*, and *Staphylococcus aureus*. The nanoparticles exhibited an average diameter of 51 nm. However, nanoparticles synthesized using a 1:1 ratio of flower extract and precursor salt exhibited better antibacterial activity, with inhibition zones of 5 mm (Escherichia coli), 6 mm (Klebsiella pneumoniae), 4 mm (*Pseudomonas aeruginosa*), and 3 mm (*Staphylococcus aureus*), respectively [156]. Shabbir et al. (2023) successfully synthesized uniformly spherical Fe_2O_3 nanoparticles using *Madhuca indica* leaf extract and $FeSO_4$ solution at 37 °C for 24 h. The nanoparticles exhibited a size range of 50 to 60 nm. The synthesized nanoparticles exhibited effective free radical scavenging activity at a concentration of 1000 μg/mL, along with notable anti-inflammatory and anti-diabetic effects via inhibition of the α-amylase enzyme in a concentration-dependent manner (IC_{50}: 73.3% at 1000 μL/mL) [155]. Lakshminarayanan et al. (2021) conducted a study using leaf extract of *Bauhinia tomentosa* for the synthesis of cluster-like Fe_2O_3 nanoparticles with an average diameter of 70 nm. The synthesized nanoparticles were subsequently employed in the production of 1,3-diolein [157].

5.2.4. Titanium Dioxide Nanoparticles

Titanium dioxide, a white inorganic compound, has been extensively used in water purification due to its catalytic properties. Titania (TiO_2) nanoparticles are well known for their optical and dielectric properties, chemical stability, non-toxicity, and strong oxidative capability. Titania exists in three polymorphic forms, namely anatase, rutile, and brookite. Among these, anatase is more commonly preferred in green synthesis due to its relatively higher stability and enhanced photocatalytic activity [197]. Bopape et al. (2023) prepared titanium dioxide nanoparticles using different concentrations of *Commelina benghalensis* plant extract, 10–30 g, and reported that on increasing the plant extract's concentration, much smoother and distinct spherical nanoparticles were observed with a size range of 30–200 nm. They also noted their photodegradation efficiency for MB (65%) and SSX (82.4%) [167]. Rathi et al. (2023) reported the synthesis of spherical (15–28 nm) TiO_2 nanoparticles using flower extract of *Caesalpinia pulcherrima*, irregular and near-spherical TiO_2 nanoparticles using peel extract of *Manihot esculenta*, and agglomerated quasi-spherical TiO_2 nanoparticles using leaf extract of *Nervilia aragona*. These nanoparticles were effectively applied as catalysts for the degradation of methylene blue and also exhibited antimicrobial activity against *Pseudomonas aeruginosa*, *Escherichia coli*, *Candida albicans*, and *Staphylococcus aureus* [198]. Mbenga et al. (2023) recently reported the synthesis of TiO_2 nanoparticles using leaf extract of *Tulbaghia violacea*. The resulting nanoparticles exhibited rectangular and irregular morphologies and demonstrated moderate antioxidant and cytotoxic activities against HEK 293 and HeLa cell lines [168].

Sethy et al. (2020) synthesized titanium dioxide nanoparticles using leaf extract of *Syzygium cumini* for stabilization and capping at room temperature over 8 h. The resulting nanoparticles were employed as catalysts for the photocatalytic removal of lead (Pb) from water bodies in industrial areas [199]. Aravind et al. (2021) reported that titanium dioxide nanoparticles synthesized using jasmine flower extracts exhibited superior photodegradation efficiency of methylene blue (92%) compared to titanium dioxide nanoparticles prepared via the hydrothermal (chemical) method [200]. Balaraman et al. (2022) reported the plant-mediated synthesis of titanium dioxide nanoparticles using an aqueous extract of *Sargassum myriocystum*, yielding nanoparticles with cubic, square, and spherical morphologies and a particle size distribution of 50–90 nm. These nanoparticles exhibited effective antibiofilm activity against *Proteus vulgaris*, *Staphylococcus epidermidis*, *Staphylococcus aureus*, *Escherichia coli*, *Pseudomonas aeruginosa*, and *Klebsiella pneumoniae*, as well as larvicidal activity against *Aedes aegypti* and *Culex quinquefasciatus*, and photocatalytic degradation of methylene blue [201]. Mohany et al. (2023) synthesized spherical titanium dioxide nanoparticles using plant extract of *Solanum surattense*, with particle sizes ranging from 10 to 80 nm. The color change of the reaction mixture from light green to whitish-brown after continuous stirring at ambient temperature for 24 h confirmed the formation of nanoparticles. These nanoparticles were found to be effective in reducing seizure duration, as demonstrated in maximal electroshock-induced epilepsy (MES) and pentylenetetrazole (PTZ) models. Additionally, they exhibited significant cytotoxic activity against the THP-1 cell line at a concentration of 80 μg/mL [173].

5.2.5. Magnesium Oxide Nanoparticles

Magnesium oxide nanoparticles are amongst the most widely studied metal oxide nanoparticles because of their high stability, low cost, and wide band gap. To date, they have been employed in a wide range of applications, including water purification, fuel additives, sensing, adsorption, and antimicrobial applications [180]. Magnesium oxide (MgO) nanoparticles have also been extensively utilized in biomedical applications, including the treatment of stomach ailments, incorporation into blood collection devices, relief of heartburn, capsule coatings, and bone regeneration, among others [202]. Muhaymin et al. (2024) utilized fruit extract of *Hyphaene thebaica* for the synthesis of magnesium oxide nanoparticles with a spherical morphology and an average diameter of 32.6 ± 5 nm. The nanoparticles showcased remarkable photocatalytic activity of methylene blue dye (98% after 110 min) [180]. Younis et al. (2021) synthesized MgO nanoparticles by employing flower extracts of *Rosa floribunda* charisma and obtained polyhedral-shaped particles of 35.25–55.14 nm size range as confirmed by HR-TEM images. The synthesized nanoparticles exhibited antioxidant activity against xanthine oxidase, hydroxyl, nitric oxide, and superoxide radicals, with IC_{50} values of 15.9 μg/mL, 31.9 μg/mL, 52.9 μg/mL, and 26.2 μg/mL, respectively, using ascorbic acid as the control. The nanoparticles also exhibited antiaging activity in dose-dependent manner by inhibition of enzymes like tyrosinase (IC_{50}: 158.6 ± 5.20 μg/mL), hyaluronidase (IC_{50}: 191.4 ± 5.68 μg/mL), elastase (IC_{50}: 82.5 ± 2.93 μg/mL), hyaluronidase (IC_{50}: 191.4 ± 5.68 μg/mL) and collagenase (IC_{50}: 58.7 ± 1.66 μg/mL). Moreover, the nanoparticles were found to be antibacterial against three skin pathogens, *P. aeruginosa* (MIC: 31.25 μg/mL), *Streptococcus pyogenes* (MIC: 7.81 μg/mL), and *Staphylococcus epidermis* (MIC: 15.63 μg/mL). Additionally, the nanoparticles exhibited anti-biofilm activity against the aforementioned bacterial strains, with minimum inhibitory concentrations for biofilm formation of 7.81, 1.95, and 1.95 μg/mL, respectively [175].

Hirphaye et al. (2023) demonstrated the synthesis of magnesium oxide (MgO) nanoparticles using female flowers of *Hagenia abyssinica*. The process was conducted at pH 12 and 60 °C for 120 min. SEM analysis revealed that the biogenic nanoparticles were spherical in shape, with particle sizes ranging from 10 to 40 nm. Authors also discussed how different parameters such as duration of reaction, concentration of precursor salt, temperature, volume of plant extract, and pH play an important role in the biogenic formation of MgO nanoparticles and showcased the antimicrobial potential of the obtained nanoparticles against *Escherichia coli* and *Staphylococcus aureus* with their zone of inhibition recorded to be 15 ± 0 mm and 27 ± 0.28 mm, respectively [67]. Abinaya et al. (2023) described the synthesis of magnesium oxide nanoparticles using leaf extract of *Psidium guajava*, which exhibited a spherical morphology and an average particle size of 85.8 nm. The nanoparticles were evaluated for their larvicidal and antibacterial activities [177]. Likewise, Dinga et al. (2022) reported the synthesis of magnesium oxide nanoparticles using seed extract of Melia azedarach at varying extract volumes of 20, 10, and 5 mL. The authors observed that, although all nanoparticles were spherical in shape, their edges became more defined with increasing seed extract volume, while particle size decreased from 73.29 nm to 62.4 nm and 44.29 nm with the use of 5, 10, and 20 mL of seed extract, respectively. Moreover, these nanoparticles were found to be effective as larvicidal and antioxidant agents [174].

5.3. Carbon-Based Nanoparticles

The emergence of carbon nanoparticles has gained significant interest due to their extensive applications in modern technologies, including water purification, energy storage materials, catalysis, electronics, biofuels, and bioimaging. Carbon nanoparticles comprise a diverse class of nanomaterials, including nanodiamonds (NDs), graphene and its derivatives, carbon nanotubes (CNTs), carbon nanohorns (CNHs), carbon nanofibers (CNFs), carbon-based quantum dots (CQDs), graphene oxide, and fullerenes [203, 204]. Carbon nanotubes are classified into single-walled and multi-walled types based on the number of graphene layers in their structure. Their dimensions and morphology can be tailored by modifying synthesis conditions, such as reaction gases, temperature, precursors, and catalysts, during biosynthesis. With the increasing popularity of carbon nanotubes in biomedical applications, green synthesis has become essential for their cost-effective large-scale production. This one-step synthesis approach eliminates the need for conventional chemical catalysts, which are often limited or hazardous, and instead utilizes plant extracts as eco-friendly alternatives. Quantum dots (QDs) exhibit high luminescence, strong photostability, low toxicity, chemical inertness, and good biocompatibility compared to other carbon nanomaterials, giving them a significant advantage in biomedical applications [205].

Carbon quantum dots can function simultaneously as nanocarriers and imaging agents in drug delivery systems, as reported by Ross (2020) [206]. Nanodiamonds were first discovered incidentally during detonation processes. Their core lattice exhibits sp^3 hybridization, while sp^2 hybridization is typically present at the surface. Due to their low toxicity and fluorescence-emitting properties, nanodiamonds are considered highly suitable for applications in diagnostics and bioimaging. Nanodiamonds include nanocrystalline diamonds (NCD) with a particle size measuring below 100 nm and ultrananocrystalline diamond (UNCD) with a particle size measuring below 10 nm [205]. Liu et al. administered nanodiamonds to a preadipocyte fibroblast cell line (3T3-L1) and a lung adenocarcinoma epithelial cell line (A549). Cell imaging studies have demonstrated that nanodiamonds do not induce cytotoxic effects, even with prolonged exposure, and do not interfere with essential cellular processes such as cell division, differentiation, or gene expression. These properties make them highly suitable for tracking and identifying both stem cells and cancer cells [207]. In a related study by Perevedentseva et al., the uptake of nanodiamonds was investigated in both non-cancerous and cancerous cell lines, including HFL1 fibroblast-like human fetal lung cells, BEAS-2B non-tumorigenic human bronchial epithelial cells, and A549 lung adenocarcinoma cells, and subsequently evaluated [208]. However, the green synthesis of nanodiamonds remains highly limited to date. In contrast, graphene, which possesses a honeycomb-like structure, has attracted considerable interest in green chemistry, as several studies have reported its synthesis using biological agents, as described by Kim et al., Ruan et al., and Gurunathan et al. [209–211].

Graphene nanomaterials, owing to the presence of carboxyl (–COOH) functional groups on their surface, can form strong interactions with nucleic acid bases, enabling their effective use as biosensors for DNA and RNA. Their potential applications as nanocarriers for anticancer drugs have also been extensively explored [205]. Qu et al. (2016) described the green fabrication of carbon nanotubes using Brassica juncea extracts. Further analysis revealed that the carbon nanotubes possess a hollow core, with an outer diameter of approximately 80 nm [212]. Recently, Singh et al. (2024) synthesized carbon nanoparticles utilizing different plants, including *Azadirachta indica, Pisidium guajava, Mangifera indica, Bergera koenigii*, and *Syzygium cumini* leaves extract. Based on scanning electron microscopy (SEM) analysis, all nanoparticles were observed to exhibit a quasi-spherical morphology with varying particle sizes. The average size distribution was around 23.5 nm, 32 nm, 33 nm, 42.5 nm, and 37 nm for nanoparticles synthesized from *Syzygium cumini, Mangifera indica, Azadirachta indica, Bergera koenigii*, and *Pisidium guajava*, and *Holy basil*, respectively. The obtained nanoparticles exhibited remarkable antioxidant properties [213].

Tripathi et al. (2017) observed the hollow rectangular cross-section carbon nanobelts and single-walled nanotubes by utilizing several plants like *Cynodon dactylon*, *Rosa, Azadirachta indica*, and *Juglans regia* leaf extracts. The nanomaterials were further characterized by using HR-TEM, Raman, and IR spectroscopy [214]. However, green synthesis routes for carbon nanomaterials often require high temperatures and prolonged reaction times. To address this high energy consumption limitation, Arizaga et al. (2022) fabricated carbon nanomaterials using tomato extracts. Tomato pulp was mixed with aluminum nitrate nonahydrate ($Al(NO_3)_3{\cdot}9H_2O$) and magnesium nitrate hexahydrate ($Mg(NO_3)_2{\cdot}6H_2O$) at pH 8.5, followed by calcination at 60 °C. FESEM analysis confirmed a semi-spherical morphology of the nanoparticles, which were subsequently investigated for their fluorescent response toward metal cations and photothermal activity [215]. Nadeem et al. (2022) synthesized spherical carbon nanoparticles using linseed, olive, and mustard seed oils, yielding particle sizes of 57 nm, 24 nm, and 18 nm, respectively. The nanoparticles produced were assessed for their antibacterial efficacy against Staphylococcus aureus, Proteus refrigere, Streptococcus haemolyticus, and Pseudomonas aeruginosa and showed excellent results [216]. Damera et al. (2020) described the production of carbon nanoparticles utilizing Eucalyptus twigs and ammonium chloride. The nanoparticles were multi-emissive and referred to as light blue, blue, green, and red carbon nanoparticles. Light blue carbon nanoparticles exhibited remarkable sensing capabilities toward Brilliant Blue (BB), a toxic synthetic food colorant [217].

6. Application in Energy

With the rapid rise in the world population, the exhaustion of fossil fuel resources has become a major global challenge. Simultaneously, environmental damage caused by fossil fuel emissions has motivated scientists to develop alternative energy sources that are climate-resilient and capable of meeting the demands of a growing population. In the context of the global petroleum crisis, bioenergy has emerged as a clean energy source with a lower carbon footprint [218]. Biofuels are derived from biomass and can be classified into four generations based on their source. First-generation biofuels are produced from edible food crops and include biodiesel, biogas, and bioalcohols. Second-generation biofuels are derived from non-edible feedstocks, such as lignocellulosic biomass, and include products like cellulosic ethanol and dimethylfuran. Third-generation biofuels, also referred to as “algae fuels” or “oilgae,” are derived from algae and include products such as biodiesel, butanol, and propanol. Finally, fourthgeneration biofuels are produced using genetically engineered algae and include biofuels such as biobutanol, biohydrogen, and biomethane [219]. A shift toward renewable biofuels has significantly reduced greenhouse gas emissions and the overall carbon footprint. Biofuels, including biodiesel, biogas, bioethanol, biomethane, and biohydrogen, have been extensively investigated as alternatives to reduce dependence on petroleum-derived fuels [218]. The conversion of biomass into biofuels is primarily achieved through processes such as fermentation, transesterification, and thermochemical and biochemical conversion. Although biofuel production is relatively costly, limiting its commercialization, implementing advanced technologies to reduce production costs and improve yields is essential for achieving a low-carbon economy. To address this challenge, many researchers have explored the use of nanotechnology to enable more cost-effective and sustainable production of bioenergy and biofuels.

Although several studies report that plant-mediated synthesis reduces reagent use, simplifies processing, and lowers laboratory energy consumption, there is a scarcity of rigorous techno-economic analyses or cost comparisons that directly quantify overall cost benefits relative to chemically synthesized catalysts or conventional processes at scale. Therefore, while green synthesis offers a promising approach for reducing material and energy inputs, its overall impact on total production cost and commercial feasibility remains to be fully established through dedicated techno-economic analyses and large-scale studies [10,19,220]. Nanomaterials, owing to their exceptional and unique properties—such as high chemical reactivity, excellent thermal and electrical conductivity, large surface area, optical activity, and strong chemical stability—have emerged as promising materials for enhancing biofuel production [219]. Nanoparticles such as calcium oxide (CaO) and magnesium oxide (MgO) can serve as heterogeneous catalysts in transesterification reactions for biodiesel production, as reported by Zhang et al. [221]. Alternatively, they can act as carriers for enzyme immobilization to enhance catalytic performance. The use of nanocatalysts in transesterification for biodiesel production has gained significant attention due to their small size, high reactivity, low toxicity, and excellent reusability, as demonstrated by Qiu et al. [222]. Examples of such nanocatalysts include MgO, SrO, ZnO, and CaO, while substances like Al2O3 are employed to enhance catalytic properties. In a study by Saka et al. (2022), ZnO nanoparticles were used as catalysts for the transesterification of *Mangifera indica* seed oil for biofuel production. The authors reported a maximum biodiesel yield of 85% under optimized conditions, including 10 mL of nanocatalyst, a reaction temperature of 50 °C, a methanol-to-oil (M/O) molar ratio of 7:2, and a reaction time of 1 h [223].

Despite extensive research on the application of various nanoparticles in biofuel production processes, certain limitations persist, as many of these nanoparticles are synthesized through chemical routes such as sonochemical methods, sol–gel processes, chemical precipitation, and solid-state thermal decomposition. These processes contribute significantly to environmental impact due to their requirement for prolonged reaction times, elevated temperatures, and high-pressure conditions. Therefore, the synthesis of nanoparticles via green routes, along with their application in bioenergy production, has become an urgent and important area of research. However, this field of research is still in its early stages, with only a limited number of studies reported in recent years. In a newly conducted study published by Arun et al., (2023), copper oxide nanoparticles were derived from the flower extracts of Bombax ceiba and was successfully used as reusable heterogeneous catalyst to produce biodiesel from *Bombax ceiba* oil feedstock. The findings demonstrated a biodiesel yield of 95.6% under optimized conditions, including a nanoparticle concentration of 3.5 wt%, a reaction time of 50 min, a reaction temperature of 60 °C, and a methanol-to-oil molar ratio of 11:1. Additionally, the produced fuel exhibited significantly reduced harmful emissions [224].

As described by Cholapandian et al. (2022), calcium oxide nanoparticles were synthesized using leaf extract of *Acalypha indica* and further evaluated for their catalytic role in biodiesel production. The study reported a biodiesel yield of 94.74% under optimized conditions, including a reaction temperature of 63.7 °C, a methanol-to-oil (M/O) molar ratio of 11.8:1, a catalyst concentration of 2.4 wt%, and a reaction time of 70 min [225]. Similarly, Changmai et al. (2021) synthesized magnetic nanoparticles from *Citrus sinensis* peel ash and employed them for biodiesel production from waste cooking oil. They achieved a biodiesel yield of 98% under optimized conditions, including a reaction time of 3 h, a methanol-to-oil (M/O) molar ratio of 6:1, a temperature of 65 °C, and a catalyst loading of 6%. Moreover, the nanocatalysts (CSPA@Fe_3O_4) were found to be reusable and reactive up to nine consecutive cycles, adding to their sustainability [226]. Yildirim and Ozkaya (2024) investigated the production of biohydrogen through plant-mediated synthesis of nickel and cobalt ferrite nanoparticles. The nanoparticles were synthesized using olive leaves and $Fe(NO_3)_3.9H_2O$ and $NiCl_2.6H_2O$ as precursors for nickel ferrite nanoparticles and $Fe(NO_3)_2.9H_2O$ and $Co(NO_3)_2.6H_2O$ as precursors for the cobalt ferrite nanoparticles. The process was carried out over a period of 2 h at a temperature of 200 °C. SEM analysis revealed mean particle sizes of 292 nm and 385 nm for $CoFe_2O_4$ and $NiFe_2O_4$ nanoparticles, respectively. The authors observed that both nanoparticles enhanced the yield of dark fermentation, with nickel ferrite nanoparticles increasing biohydrogen production by 47%, while cobalt ferrite nanoparticles improved it by 41% [218]. Subramani et al. (2024) synthesized silver nanoparticles using the *Azadirachta indica* leaf extract and silver nitrate solution by constant stirring at 70 °C until the colorless reaction mixture turned brown. The synthesized nanoparticles exhibited a spherical morphology with an average size of 13 nm. *Chlorella* sp. treated with these nanoparticles showed an enhanced growth rate and a higher biohydrogen yield of 10.8 mmol L^{-1}. In contrast, untreated cells displayed a lower growth rate and a significantly reduced biohydrogen yield of 0.003 mmol L^{-1} [227].

7. Conclusions and Future Prospects

Due to rising energy demands and the depletion of fossil fuel reserves, biofuels have emerged as a promising alternative to sustain the global bioeconomy. However, biofuel production has certain limitations, which can potentially be addressed through the application of nanotechnology. Nanotechnology has emerged as a promising approach to enhance biofuel production. Among the various strategies, plant-extract-mediated nanocatalysts have gained considerable attention due to their effectiveness, sustainability, and eco-friendly nature. Plant extracts contain diverse phytochemicals, including flavonoids and polyphenols, which can reduce and stabilize metal ions during nanoparticle synthesis [220,228]. These green-synthesized nanoparticles have shown excellent catalytic properties, particularly metallic (Ag, Cu, Ni) and metal oxide nanoparticles (TiO_2, ZnO, Fe_3O_4), which have enhanced processes such as biodiesel transesterification, bioethanol production, and biogas upgrading [19,228]. Optimal synthesis parameters—such as reaction temperature, pH, extract-to-metal precursor ratio, and reaction time—play a critical role in tuning nanoparticle characteristics, which directly influence catalytic efficiency. In addition to their role in bioenergy, these nanomaterials have also exhibited versatility in biomedical, environmental, and agricultural applications [220]. Therefore, plant-based nanocatalysts offer a promising approach for the development of sustainable and multifunctional materials, supporting the transition toward a greener bioeconomy.

Despite these encouraging advances, significant research gaps persist. The lack of standardized synthesis protocols leads to inconsistent nanoparticle properties and limited reproducibility across studies. Moreover, the mechanistic understanding of phytochemical interactions during nanoparticle nucleation and growth remains limited. Comprehensive studies on the toxicity, biocompatibility, and environmental impact of these nanomaterials remain scarce, hindering their safe translation into large-scale use [55]. Furthermore, the scalability of green synthesis processes and their integration into real-world biofuel production systems require deeper exploration [229].

Further studies are required to develop standardized extraction and synthesis protocols to ensure reproducibility and scalability, to elucidate phytochemical-mediated reaction mechanisms through in situ analytical and computational approaches, and to bridge the gap between laboratory-scale catalytic performance and industrial-scale biofuel applications. Detailed life-cycle and toxicity assessments are essential to ensure the environmental and human safety of these nanomaterials. Research should also focus on utilizing invasive or toxic plant species as alternative bioresources for nanoparticle synthesis, thereby reducing reliance on edible or medicinal plants. Furthermore, enhancing reusability, catalytic stability, and active-site density will be crucial for maximizing performance and ensuring the long-term sustainability of nanotechnology-assisted biofuel production.

List of Abbreviations

0D	Zero Dimensional
AChE	Acetylcholinesterase
AFM	Atomic Force Microscopy
AgNPs	Silver nanoparticles
BB	Brilliant Blue
CNFs	Carbon nanofibers
CNHs	Carbon nanohorns
CNTs	Carbon nanotubes
CQDs	Carbon quantum dots
DMAPP	Dimethylallyl pyrophosphate
DPPH	2,2-Diphenyl-1-picrylhydrazyl
FCC	Face-centered cubic
FESEM	Field Emission Scanning Electron Microscopy
FPP	Farnesyl pyrophosphate
FRAP	Ferric Reducing Antioxidant Power
FTIR	Fourier transform infrared spectroscopy
GAE	Gallic acid equivalents
GGPP	Geranylgeranyl pyrophosphate
GPP	Geranyl pyrophosphate
HFF-1	Human foreskin fibroblast cell line
HRLC–MS	High-resolution liquid chromatography–mass spectrometry

2026, Vol. 2, Article ID. 2026.0024
https://doi.org/10.69709/SusProc.2026.171930

HR-TEM	High Resolution Transmission Electron Microscopy
IGC	Inert gas condensation
MB	Methylene Blue
MCF-7	Human breast cancer cell line
MEP	2-C-Methyl-D-erythritol-4-phosphate pathway
MNPs	Magnetic nanoparticles
MVA	Mevalonate pathway
NDs	Nanodiamonds
NPs	Nanoparticles
PdNPs	Palladium nanoparticles
PtNPs	Platinum nanoparticles
QDs	Quantum dots
RSM	Response Surface Methodology
SDS-PAGE	Sodium dodecyl sulphate–polyacrylamide gel electrophoresis
SEM	Scanning Electron Microscopy
SIBs	Sodium-ion batteries
SPR	Surface plasmon resonance
SSX	Sulfasalazine
TEM	Transmission electron microscopy
UV–Vis	Ultraviolet–visible spectroscopy
XRD	X-ray diffraction

Author Contributions

Conceptualization, G.S.; Writing—original draft: S.K., B.V., D.S., S.R., P.S.; Writing—review & editing: T.S., G.S.; visualization: P.S. All authors have read and agreed to the published version of the manuscript.

Conflicts of Interest

The authors declare no conflicts of interest.

Funding

The study did not receive any external funding and was conducted using only institutional resources.

Acknowledgments

The authors thank their respective institutes, "Institute of Management Studies, Ghaziabad (University Course Campus), Amity Institute of Biotechnology, Amity University, Manipal School of Life Sciences, Manipal Academy of Higher Education, and JMS Institute of Technology (JMS IT), India" for supporting the preparation of this review article through their combined efforts.

AI Declaration

The authors confirm that no AI tools were used to generate the content of this manuscript. No AI-based tools were used to create the figures. The images have been created using MS PowerPoint and Canva.

Supplementary Materials

Supplementary material associated with this article has been published online and is available at: https://doi.org/10.69709/SusProc.2026.171930.

References

[1] Khan, F.; Shariq, M.; Asif, M.; Siddiqui, M.A.; Malan, P.; Ahmad, F. Green Nanotechnology: Plant-Mediated Nanoparticle Synthesis and Application. *Nanomaterials* **2022**, *12*, 673. [CrossRef]

[2] Mekuye, B.; Abera, B. Nanomaterials: An Overview of Synthesis, Classification, Characterization, and Applications. *Nano Sel.* **2023**, *4*, 486–501. [CrossRef]

[3] Paras; Yadav, K.; Kumar, P.; Teja, D.R.; Chakraborty, S.; Chakraborty, M.; Mohapatra, S.S.; Sahoo, A.; Chou, M.M.C.; Liang, C.-T.; et al. A Review on Low-Dimensional Nanomaterials: Nanofabrication, Characterization and Applications. *Nanomaterials* **2022**, *13*, 160. [CrossRef]

[4] Baig, N.; Kammakakam, I.; Falath, W. Nanomaterials: A Review of Synthesis Methods, Properties, Recent Progress, and Challenges. *Mater. Adv.* **2021**, *2*, 1821–1871. [CrossRef]

[5] Ali, A.; Moradian, J.M.; Naveed, A.; Zhang, S.; Tahir, M.H.; Shehzad, K.; Sillanpää, M. Progress in Cathode Materials for Rechargeable Zinc-Ion Batteries: From Inorganic and Organic Systems to Hybrid Frameworks and Biomass-Derived Innovations. *Prog. Mater. Sci.* **2025**, *156*, 101543. [CrossRef]

[6] Byakodi, M.; Shrikrishna, N.S.; Sharma, R.; Bhansali, S.; Mishra, Y.; Kaushik, A.; Gandhi, S. Emerging 0D, 1D, 2D, and 3D Nanostructures for Efficient Point-of-Care Biosensing. *Biosens. Bioelectron. X* **2022**, *12*, 100284. [CrossRef]

[7] Joudeh, N.; Linke, D. Nanoparticle Classification, Physicochemical Properties, Characterization, and Applications: A Comprehensive Review for Biologists. *J. Nanobiotechnol.* **2022**, *20*, 262. [CrossRef]

[8] Iravani, S. Green Synthesis of Metal Nanoparticles Using Plants. *Green Chem.* **2011**, *13*, 2638–2650. [CrossRef]

[9] Khan, M.F.; Khan, M.A. Plant-Derived Metal Nanoparticles (PDMNPs): Synthesis, Characterization, and Oxidative Stress-Mediated Therapeutic Actions. *Future Pharmacol.* **2023**, *3*, 252–295. [CrossRef]

[10] Naseem, K.; Aziz, A.; Khan, M.E.; Ali, S.; Khalid, A. Bioinorganic Metal Nanoparticles and Their Potential Applications as Antimicrobial, Antioxidant and Catalytic Agents: A Review. *Rev. Inorg. Chem.* **2025**, *45*, 207–236. [CrossRef]

[11] Al-Harbi, N.; Abd-Elrahman, N.K. Physical Methods for Preparation of Nanomaterials, Their Characterization and Applications: A Review. *J. Umm Al-Qura Univ. Appl. Sci.* **2025**, *11*, 356–377. [CrossRef]

[12] Altammar, K.A. A Review on Nanoparticles: Characteristics, Synthesis, Applications, and Challenges. *Front. Microbiol.* **2023**, *14*, 1155622. [CrossRef]

[13] Kumari, S.; Raturi, S.; Kulshrestha, S.; Chauhan, K.; Dhingra, S.; András, K.; Thu, K.; Khargotra, R.; Singh, T. A Comprehensive Review on Various Techniques Used for Synthesizing Nanoparticles. *J. Mater. Res. Technol.* **2023**, *27*, 1739–1763. [CrossRef]

[14] Filho, S.A.; dos Santos, M.S.; dos Santos, O.A.L.; Backx, B.P.; Soran, M.-L.; Opriş, O.; Lung, I.; Stegarescu, A.; Bououdina, M. Biosynthesis of Nanoparticles Using Plant Extracts and Essential Oils. *Molecules* **2023**, *28*, 3060. [CrossRef]

[15] Alvand, Z.M.; Aghamir, F.; Rajabi, H.R.; Rafati, H. Evaluation of Biological Properties of Green-Synthesized ZnSe Quantum Dots Using Microfluidic Systems: A Novel Approach to Enhancing Antibacterial Activity. *Appl. Surf. Sci. Adv.* **2025**, *29*, 100812. [CrossRef]

[16] Kanchi, S.; Ahmed, S. (Eds.) *Green Metal Nanoparticles: Synthesis, Characterization and Their Applications*; Wiley-Scrivener: Hoboken, NJ, USA, 2018. [CrossRef]

[17] Koul, B.; Poonia, A.K.; Yadav, D.; Jin, J.-O. Microbe-Mediated Biosynthesis of Nanoparticles: Applications and Future Prospects. *Biomolecules* **2021**, *11*, 886. [CrossRef]

[18] Singh, H.; Desimone, M.F.; Pandya, S.; Jasani, S.; George, N.; Adnan, M.; Aldarhami, A.; Bazaid, A.S.; Alderhami, S.A. Revisiting the Green Synthesis of Nanoparticles: Uncovering Influences of Plant Extracts as Reducing Agents for Enhanced Synthesis Efficiency and Its Biomedical Applications. *Int. J. Nanomed.* **2023**, *18*, 4727–4750. [CrossRef]

[19] Ingle, A.P.; Chandel, A.K.; Philippini, R.; Martiniano, S.E.; da Silva, S.S. Advances in Nanocatalysts Mediated Biodiesel Production: A Critical Appraisal. *Symmetry* **2020**, *12*, 256. [CrossRef]

[20] Arya, I.; Poona, A.; Dikshit, P.K.; Pandit, S.; Kumar, J.; Singh, H.N.; Jha, N.K.; Rudayni, H.A.; Chaudhary, A.A.; Kumar, S. Current Trends and Future Prospects of Nanotechnology in Biofuel Production. *Catalysts* **2021**, *11*, 1308. [CrossRef]

[21] Mustapha, T.; Misni, N.; Ithnin, N.R.; Daskum, A.M.; Unyah, N.Z. A Review on Plants and Microorganisms Mediated Synthesis of Silver Nanoparticles, Role of Plants Metabolites and Applications. *Int. J. Environ. Res. Public Health* **2022**, *19*, 674. [CrossRef]

[22] Ovais, M.; Khalil, A.T.; Islam, N.U.; Ahmad, I.; Ayaz, M.; Saravanan, M.; Shinwari, Z.K.; Mukherjee, S. Role of Plant Phytochemicals and Microbial Enzymes in Biosynthesis of Metallic Nanoparticles. *Appl. Microbiol. Biotechnol.* **2018**, *102*, 6799–6814. [CrossRef]

[23] Mittal, A.K.; Chisti, Y.; Banerjee, U.C. Synthesis of Metallic Nanoparticles Using Plant Extracts. *Biotechnol. Adv.* **2013**, *31*, 346–356. [CrossRef]

[24] Moradialvand, Z.; Parseghian, L.; Rajabi, H.R. Green Synthesis of Quantum Dots: Synthetic Methods, Applications, and Toxicity. *J. Hazard. Mater. Adv.* **2025**, *18*, 100697. [CrossRef]

[25] Pradeep, M.; Kruszka, D.; Kachlicki, P.; Mondal, D.; Franklin, G. Uncovering the Phytochemical Basis and the Mechanism of Plant Extract-Mediated Eco-Friendly Synthesis of Silver Nanoparticles Using Ultra-Performance Liquid Chromatography Coupled with a Photodiode Array and High-Resolution Mass Spectrometry. *ACS Sustain. Chem. Eng.* **2021**, *10*, 562–571. [CrossRef]

[26] Islam, A.; Rahat, I.; Anurag; Rejeeth, C.; Sharma, D.; Sharma, A. Recent Advances on Plant-Based Bioengineered Nanoparticles Using Secondary Metabolites and Their Potential in Lung Cancer Management. *J. Futur. Foods* **2025**, *5*, 1–20. [CrossRef]

[27] Gopinath, K.; Kumaraguru, S.; Bhakyaraj, K.; Mohan, S.; Venkatesh, K.S.; Esakkirajan, M.; Kaleeswarran, P.; Alharbi, N.S.; Kadaikunnan, S.; Govindarajan, M.; et al. Green Synthesis of Silver, Gold and Silver/Gold Bimetallic Nanoparticles Using the *Gloriosa superba* Leaf Extract and Their Antibacterial and Antibiofilm Activities. *Microb. Pathog.* **2016**, *101*, 1–11. [CrossRef]

[28] Hemlata; Meena, P.R.; Singh, A.P.; Tejavath, K.K. Biosynthesis of Silver Nanoparticles Using *Cucumis prophetarum* Aqueous Leaf Extract and Their Antibacterial and Antiproliferative Activity against Cancer Cell Lines. *ACS Omega* **2020**, *5*, 5520–5528. [CrossRef]

[29] Wang, Z.; Fang, C.; Megharaj, M. Characterization of Iron–Polyphenol Nanoparticles Synthesized by Three Plant Extracts and Their Fenton Oxidation of Azo Dye. *ACS Sustain. Chem. Eng.* **2014**, *2*, 1022–1025. [CrossRef]

[30] Ferreyra, M.L.F.; Rius, S.P.; Casati, P. Flavonoids: Biosynthesis, Biological Functions, and Biotechnological Applications. *Front. Plant Sci.* **2012**, *3*, 222. [CrossRef]

[31] Martens, S.; Preuß, A.; Matern, U. Multifunctional Flavonoid Dioxygenases: Flavonol and Anthocyanin Biosynthesis in *Arabidopsis thaliana* L. *Phytochemistry* **2010**, *71*, 1040–1049. [CrossRef] [PubMed]

[32] Sahu, N.; Soni, D.; Chandrashekhar, B.; Satpute, D.B.; Saravanadevi, S.; Sarangi, B.K.; Pandey, R.A. Synthesis of Silver Nanoparticles Using Flavonoids: Hesperidin, Naringin and Diosmin, and Their Antibacterial Effects and Cytotoxicity. *Int. Nano Lett.* **2016**, *6*, 173–181. [CrossRef]

[33] Bose, D.; Chatterjee, S. Biogenic Synthesis of Silver Nanoparticles Using Guava (*Psidium guajava*) Leaf Extract and Its Antibacterial Activity against *Pseudomonas aeruginosa*. *Appl. Nanosci.* **2016**, *6*, 895–901. [CrossRef]

[34] Melkamu, W.W.; Bitew, L.T. Green Synthesis of Silver Nanoparticles Using *Hagenia abyssinica* (Bruce) J.F. Gmel Plant Leaf Extract and Their Antibacterial and Anti-Oxidant Activities. *Heliyon* **2021**, *7*, e08459. [CrossRef] [PubMed]

[35] Huang, Y.; Xie, F.-J.; Cao, X.; Li, M.-Y. Research Progress in Biosynthesis and Regulation of Plant Terpenoids. *Biotechnol. Biotechnol. Equip.* **2021**, *35*, 1799–1808. [CrossRef]
[36] Vavitsas, K.; Fabris, M.; Vickers, C.E. Terpenoid Metabolic Engineering in Photosynthetic Microorganisms. *Genes* **2018**, *9*, 520. [CrossRef] [PubMed]
[37] Song, J.Y.; Kim, B.S. Rapid Biological Synthesis of Silver Nanoparticles Using Plant Leaf Extracts. *Bioproc. Biosyst. Eng.* **2009**, *32*, 79–84. [CrossRef]
[38] Shankar, S.S.; Ahmad, A.; Sastry, M. Geranium Leaf Assisted Biosynthesis of Silver Nanoparticles. *Biotechnol. Prog.* **2003**, *19*, 1627–1631. [CrossRef]
[39] Pungle, R.; Nile, S.H.; Makwana, N.; Singh, R.; Singh, R.P.; Kharat, A.S. Green Synthesis of Silver Nanoparticles Using the *Tridax procumbens* Plant Extract and Screening of Its Antimicrobial and Anticancer Activities. *Oxidative Med. Cell. Longev.* **2022**, *2022*, 9671594. [CrossRef]
[40] Ahmad, N.; Sharma, S.; Alam, M.K.; Singh, V.N.; Shamsi, S.F.; Mehta, B.R.; Fatma, A. Rapid Synthesis of Silver Nanoparticles Using Dried Medicinal Plant of Basil. *Colloid Surf. B* **2010**, *81*, 81–86. [CrossRef]
[41] El-Seedi, H.R.; El-Shabasy, R.M.; Khalifa, S.A.M.; Saeed, A.; Shah, A.; Shah, R.; Iftikhar, F.J.; Abdel-Daim, M.M.; Omri, A.; Hajrahand, N.H.; et al. Metal Nanoparticles Fabricated by Green Chemistry Using Natural Extracts: Biosynthesis, Mechanisms, and Applications. *RSC Adv.* **2019**, *9*, 24539–24559. [CrossRef]
[42] Mukherjee, S.; Chowdhury, D.; Kotcherlakota, R.; Patra, S.; Bhadra, M.P.; Sreedhar, B.; Patra, C.R. Potential Theranostics Application of Bio-Synthesized Silver Nanoparticles (4-in-1 System). *Theranostics* **2014**, *4*, 316–335. [CrossRef] [PubMed]
[43] Shukla, R.; Nune, S.K.; Chanda, N.; Katti, K.; Mekapothula, S.; Kulkarni, R.R.; Welshons, W.V.; Kannan, R.; Katti, K.V. Soybeans as a Phytochemical Reservoir for the Production and Stabilization of Biocompatible Gold Nanoparticles. *Small* **2008**, *4*, 1425–1436. [CrossRef]
[44] Tavaf, Z.; Tabatabaei, M.; Khalafi-Nezhad, A.; Panahi, F.; Hosseini, A. Green Synthesis of Silver Nanoparticles by Reduced Glycated Casein Adducts: Assessment of Their Antibacterial and Antioxidant Activity against *Streptococcus mutans*. *Eur. J. Integr. Med.* **2015**, *7*, 294–302. [CrossRef]
[45] Bhattacharjee, R.R.; Das, A.K.; Haldar, D.; Si, S.; Banerjee, A.; Mandal, T.K. Peptide-Assisted Synthesis of Gold Nanoparticles and Their Self-Assembly. *J. Nanosci. Nanotechnol.* **2005**, *5*, 1141–1147. [CrossRef]
[46] Ghosh, S.; Roy, S.; Naskar, J.; Kole, R.K. Plant-Mediated Synthesis of Mono- and Bimetallic (Au–Ag) Nanoparticles: Future Prospects for Food Quality and Safety. *J. Nanomater.* **2023**, *2023*, 2781667. [CrossRef]
[47] Nortjie, E.; Basitere, M.; Moyo, D.; Nyamukamba, P. Extraction Methods, Quantitative and Qualitative Phytochemical Screening of Medicinal Plants for Antimicrobial Textiles: A Review. *Plants* **2022**, *11*, 2011. [CrossRef] [PubMed]
[48] Jaison, J.P.; Balasubramanian, B.; Gangwar, J.; James, N.; Pappuswamy, M.; Anand, A.V.; Al-Dhabi, N.A.; Arasu, M.V.; Liu, W.-C.; Sebastian, J.K. Green Synthesis of Bioinspired Nanoparticles Mediated from Plant Extracts of Asteraceae Family for Potential Biological Applications. *Antibiotics* **2023**, *12*, 543. [CrossRef]
[49] Lee, J.-E.; Jayakody, J.T.M.; Kim, J.-I.; Jeong, J.-W.; Choi, K.-M.; Kim, T.-S.; Seo, C.; Azimi, I.; Hyun, J.; Ryu, B. The Influence of Solvent Choice on the Extraction of Bioactive Compounds from Asteraceae: A Comparative Review. *Foods* **2024**, *13*, 3151. [CrossRef] [PubMed]
[50] Rani, N.; Singh, P.; Kumar, S.; Kumar, P.; Bhankar, V.; Kumar, K. Plant-Mediated Synthesis of Nanoparticles and Their Applications: A Review. *Mater. Res. Bull.* **2023**, *163*, 112233. [CrossRef]
[51] Vanlalveni, C.; Lallianrawna, S.; Biswas, A.; Selvaraj, M.; Changmai, B.; Rokhum, S.L. Green Synthesis of Silver Nanoparticles Using Plant Extracts and Their Antimicrobial Activities: A Review of Recent Literature. *RSC Adv.* **2021**, *11*, 2804–2837. [CrossRef]
[52] Khairy, T.; Amin, D.H.; Salama, H.M.; Elkholy, I.M.A.; Elnakib, M.; Gebreel, H.M.; Sayed, H.A.E. Antibacterial Activity of Green Synthesized Copper Oxide Nanoparticles against Multidrug-Resistant Bacteria. *Sci. Rep.* **2024**, *14*, 25020. [CrossRef]
[53] Suárez-López, R.; Puntes, V.F.; Bastús, N.G.; Hervés, C.; Jaime, C. Nucleation and Growth of Gold Nanoparticles in the Presence of Different Surfactants. A Dissipative Particle Dynamics Study. *Sci. Rep.* **2022**, *12*, 13926. [CrossRef]
[54] Makarov, V.V.; Love, A.J.; Sinitsyna, O.V.; Makarova, S.S.; Yaminsky, I.V.; Taliansky, M.E.; Kalinina, N.O. "Green" Nanotechnologies: Synthesis of Metal Nanoparticles Using Plants. *Acta Naturae* **2014**, *6*, 35–44. [CrossRef] [PubMed]
[55] Velidandi, A.; Dahariya, S.; Pabbathi, N.P.P.; Kalivarathan, D.; Baadhe, R.R. A Review on Synthesis, Applications, Toxicity, Risk Assessment and Limitations of Plant Extracts Synthesized Silver Nanoparticles. *NanoWorld J.* **2020**, *6*, 35–60. [CrossRef]
[56] Nisha; Sachan, R.S.K.; Singh, A.; Karnwal, A.; Shidiki, A.; Kumar, G. Plant-Mediated Gold Nanoparticles in Cancer Therapy: Exploring Anti-Cancer Mechanisms, Drug Delivery Applications, and Future Prospects. *Front. Nanotechnol.* **2024**, *6*, 1490980. [CrossRef]
[57] Adeyemi, J.O.; Oriola, A.O.; Onwudiwe, D.C.; Oyedeji, A.O. Plant Extracts Mediated Metal-Based Nanoparticles: Synthesis and Biological Applications. *Biomolecules* **2022**, *12*, 627. [CrossRef]
[58] Rajput, S.; Kumar, D.; Agrawal, V. Green Synthesis of Silver Nanoparticles Using Indian Belladonna Extract and Their Potential Antioxidant,

Anti-Inflammatory, Anticancer and Larvicidal Activities. *Plant Cell Rep.* **2020**, *39*, 921–939. [CrossRef]
[59] Muthu, K.; Priya, S. Green Synthesis, Characterization and Catalytic Activity of Silver Nanoparticles Using *Cassia auriculata* Flower Extract Separated Fraction. *Spectrochim. Acta Part A Mol. Biomol. Spectrosc.* **2017**, *179*, 66–72. [CrossRef]
[60] Miranda, A.; Akpobolokemi, T.; Chung, E.; Ren, G.; Raimi-Abraham, B.T. pH Alteration in Plant-Mediated Green Synthesis and Its Resultant Impact on Antimicrobial Properties of Silver Nanoparticles (AgNPs). *Antibiotics* **2022**, *11*, 1592. [CrossRef]
[61] Jeevanandam, J.; Chan, Y.S.; Danquah, M.K. Effect of pH Variations on Morphological Transformation of Biosynthesized MgO Nanoparticles. *Part. Sci. Technol.* **2020**, *38*, 573–586. [CrossRef]
[62] Lee, K.X.; Shameli, K.; Mohamad, S.E.; Yew, Y.P.; Isa, E.D.M.; Yap, H.-Y.; Lim, W.L.; Teow, S.-Y. Bio-Mediated Synthesis and Characterisation of Silver Nanocarrier, and Its Potent Anticancer Action. *Nanomaterials* **2019**, *9*, 1423. [CrossRef]
[63] Amjad, R.; Mubeen, B.; Ali, S.S.; Imam, S.S.; Alshehri, S.; Ghoneim, M.M.; Alzarea, S.I.; Rasool, R.; Ullah, I.; Nadeem, M.S.; et al. Green Synthesis and Characterization of Copper Nanoparticles Using *Fortunella margarita* Leaves. *Polymers* **2021**, *13*, 4364. [CrossRef]
[64] Coman, N.-A.; Berta, L.; Nicolae-Maranciuc, A.; Nicolescu, A.; Babotă, M.; Man, A.; Chicea, D.; Farczadi, L.; Jakab-Farkas, L.; Tanase, C. Green Synthesis of Platinum Nanoparticles Using Aqueous Bark Extract of *Quercus* sp. for Potential Antioxidant and Antimicrobial Applications. *BioResources* **2024**, *19*, 862. [CrossRef]
[65] Imade, E.E.; Ajiboye, T.O.; Fadiji, A.E.; Onwudiwe, D.C.; Babalola, O.O. Green Synthesis of Zinc Oxide Nanoparticles Using Plantain Peel Extracts and the Evaluation of Their Antibacterial Activity. *Sci. Afr.* **2022**, *16*, e01152. [CrossRef]
[66] Al Awadh, A.A.; Shet, A.R.; Patil, L.R.; Shaikh, I.A.; Alshahrani, M.M.; Nadaf, R.; Mahnashi, M.H.; Desai, S.V.; Muddapur, U.M.; Achappa, S.; et al. Sustainable Synthesis and Characterization of Zinc Oxide Nanoparticles Using *Raphanus sativus* Extract and Its Biomedical Applications. *Crystals* **2022**, *12*, 1142. [CrossRef]
[67] Hirphaye, B.Y.; Bonka, N.B.; Tura, A.M.; Fanta, G.M. Biosynthesis of Magnesium Oxide Nanoparticles Using *Hagenia abyssinica* Female Flower Aqueous Extract for Characterization and Antibacterial Activity. *Appl. Water Sci.* **2023**, *13*, 175. [CrossRef]
[68] Khalil, M.M.H.; Ismail, E.H.; El-Baghdady, K.Z.; Mohamed, D. Green Synthesis of Silver Nanoparticles Using Olive Leaf Extract and Its Antibacterial Activity. *Arab. J. Chem.* **2014**, *7*, 1131–1139. [CrossRef]
[69] Zheng, B.; Kong, T.; Jing, X.; Odoom-Wubah, T.; Li, X.; Sun, D.; Lu, F.; Zheng, Y.; Huang, J.; Li, Q. Plant-Mediated Synthesis of Platinum Nanoparticles and Its Bioreductive Mechanism. *J. Colloid Interface Sci.* **2013**, *396*, 138–145. [CrossRef]
[70] Ansari, M.; Ahmed, S.; Abbasi, A.; Khan, M.T.; Subhan, M.; Bukhari, N.A.; Hatamleh, A.A.; Abdelsalam, N.R. Plant Mediated Fabrication of Silver Nanoparticles, Process Optimization, and Impact on Tomato Plant. *Sci. Rep.* **2023**, *13*, 18048. [CrossRef]
[71] Nagar, N.; Devra, V. Green Synthesis and Characterization of Copper Nanoparticles Using *Azadirachta indica* Leaves. *Mater. Chem. Phys.* **2018**, *213*, 44–51. [CrossRef]
[72] Elia, P.; Zach, R.; Hazan, S.; Kolusheva, S.; Porat, Z.; Zeiri, Y. Green Synthesis of Gold Nanoparticles Using Plant Extracts as Reducing Agents. *Int. J. Nanomed.* **2014**, *9*, 4007–4021. [CrossRef]
[73] Verma, A.; Mehata, M.S. Controllable Synthesis of Silver Nanoparticles Using Neem Leaves and Their Antimicrobial Activity. *J. Radiat. Res. Appl. Sci.* **2016**, *9*, 109–115. [CrossRef]
[74] Das, P.; Ghosal, K.; Jana, N.K.; Mukherjee, A.; Basak, P. Green Synthesis and Characterization of Silver Nanoparticles Using Belladonna Mother Tincture and Its Efficacy as a Potential Antibacterial and Anti-Inflammatory Agent. *Mater. Chem. Phys.* **2019**, *228*, 310–317. [CrossRef]
[75] Riyanto; Mulwandari, M.; Asysyafiiyah, L.; Sirajuddin, M.I.; Cahyandaru, N. Direct Synthesis of Lemongrass (*Cymbopogon citratus* L.) Essential Oil-Silver Nanoparticles (EO-AgNPs) as Biopesticides and Application for Lichen Inhibition on Stones. *Heliyon* **2022**, *8*, e09701. [CrossRef]
[76] Saif, S.; Tahir, A.; Asim, T.; Chen, Y. Plant Mediated Green Synthesis of CuO Nanoparticles: Comparison of Toxicity of Engineered and Plant Mediated CuO Nanoparticles towards *Daphnia magna*. *Nanomaterials* **2016**, *6*, 205. [CrossRef]
[77] Paiva-Santos, A.C.; Herdade, A.M.; Guerra, C.; Peixoto, D.; Pereira-Silva, M.; Zeinali, M.; Mascarenhas-Melo, F.; Paranhos, A.; Veiga, F. Plant-Mediated Green Synthesis of Metal-Based Nanoparticles for Dermopharmaceutical and Cosmetic Applications. *Int. J. Pharm.* **2021**, *597*, 120311. [CrossRef]
[78] Saini, H.; Yadav, R.; Kumar, D.; Kumar, G.; Agrawal, V. *Cullen corylifolium* (L.) Medik. Seed Extract, an Excellent System for Fabrication of Silver Nanoparticles and Their Multipotency Validation against Different Mosquito Vectors and Human Cervical Cancer Cell Line. *J. Clust. Sci.* **2020**, *31*, 161–175. [CrossRef]
[79] Nadeem, A.; Sumbal; Ali, J.S.; Latif, M.; Rizvi, Z.F.; Naz, S.; Mannan, A.; Zia, M. Green Synthesis and Characterization of Fe, Cu and Mg Oxide Nanoparticles Using *Clematis orientalis* Leaf Extract: Salt Concentration Modulates Physiological and Biological Properties. *Mater. Chem. Phys.* **2021**, *271*, 124900. [CrossRef]
[80] Unnikrishnan, G.; Joy, A.; Megha, M.; Kolanthai, E.; Senthilkumar, M. Exploration of Inorganic Nanoparticles for Revolutionary Drug Delivery Applications:

A Critical Review. *Nanoscale Res. Lett.* **2023**, *18*, 157. [CrossRef]

[81] Hasan, S. A Review on Nanoparticles: Their Synthesis and Types. *Res. J. Recent Sci.* **2015**, *2277*, 2502. [View Online]

[82] Gul, A.; Fozia; Shaheen, A.; Ahmad, I.; Khattak, B.; Ahmad, M.; Ullah, R.; Bari, A.; Ali, S.S.; Alobaid, A.; et al. Green Synthesis, Characterization, Enzyme Inhibition, Antimicrobial Potential, and Cytotoxic Activity of Plant Mediated Silver Nanoparticle Using *Ricinus communis* Leaf and Root Extracts. *Biomolecules* **2021**, *11*, 206. [CrossRef]

[83] Manik, U.; Nande, A.; Raut, S.; Dhoble, S. Green Synthesis of Silver Nanoparticles Using Plant Leaf Extraction of *Artocarpus heterophylus* and *Azadirachta indica*. *Results Mater.* **2020**, *6*, 100086. [CrossRef]

[84] Hudaya, I.R.; Situmorang, V.C.; Hardianto, F.A.; Putra, E.D.L.; Satria, D.; Hertriani, T.; Hartati, R.; Septama, A.W. Biofabrication of Silver Nanoparticles Using *Artocarpus heterophyllus* Leaves Extract: Characterization and Evaluation of Its Antibacterial, Antibiofilm, and Antioxidant Activities. *J. Cryst. Growth* **2024**, *644*, 127827. [CrossRef]

[85] Kumari, S.A.; Patlolla, A.K.; Madhusudhanachary, P. Biosynthesis of Silver Nanoparticles Using *Azadirachta indica* and Their Antioxidant and Anticancer Effects in Cell Lines. *Micromachines* **2022**, *13*, 1416. [CrossRef] [PubMed]

[86] Kumar, B.; Smita, K.; Cumbal, L. Biosynthesis of Silver Nanoparticles Using *Lantana camara* Flower Extract and Its Application. *J. Sol.-Gel Sci. Technol.* **2016**, *78*, 285–292. [CrossRef]

[87] Alhumaydhi, F.A. Green Synthesis of Gold Nanoparticles Using Extract of *Pistacia chinensis* and Their *In Vitro* and *In Vivo* Biological Activities. *J. Nanomater.* **2022**, *2022*, 5544475. [CrossRef]

[88] Rambau, U.; Masevhe, N.A.; Samie, A. Green Synthesis of Gold and Copper Nanoparticles by *Lannea discolor*: Characterization and Antibacterial Activity. *Inorganics* **2024**, *12*, 36. [CrossRef]

[89] Kiran, M.; Kumar, C.R.; Shwetha, U.; Onkarappa, H.; Betageri, V.; Latha, M. Green Synthesis and Characterization of Gold Nanoparticles from *Moringa oleifera* Leaves and Assessment of Antioxidant, Antidiabetic and Anticancer Properties. *Chem. Data Collect.* **2021**, *33*, 100714. [CrossRef]

[90] Patel, K.N.; Trivedi, P.G.; Thakar, M.S.; Prajapati, K.V.; Prajapati, D.K.; Sindhav, G.M. Gold Nanoparticles Synthesis Using *Gymnosporia montana* L. and Its Biological Profile: A Pioneer Report. *J. Genet. Eng. Biotechnol.* **2023**, *21*, 71. [CrossRef]

[91] Al-Radadi, N.S.; Abdullah; Faisal, S.; Alotaibi, A.; Ullah, R.; Hussain, T.; Rizwan, M.; Saira; Zaman, N.; Iqbal, M.; et al. *Zingiber officinale* Driven Bioproduction of ZnO Nanoparticles and Their Anti-Inflammatory, Anti-Diabetic, Anti-Alzheimer, Anti-Oxidant, and Anti-Microbial Applications. *Inorg. Chem. Commun.* **2022**, *140*, 109274. [CrossRef]

[92] Akpanudo, N.W.; Olabemiwo, O.M. Green Synthesis and Characterization of Copper Nanoparticles (CuNPs) and Composites (CuC) Using the *Echinochloa pyramidalis* Extract and Their Application in the Remediation of PAHs in Water. *Water Pract. Technol.* **2024**, *19*, 324–342. [CrossRef]

[93] Ghosh, M.K.; Sahu, S.; Gupta, I.; Ghorai, T.K. Green Synthesis of Copper Nanoparticles from an Extract of *Jatropha curcas* Leaves: Characterization, Optical Properties, CT-DNA Binding and Photocatalytic Activity. *RSC Adv.* **2020**, *10*, 22027–22035. [CrossRef]

[94] Viswadevarayalu, A.; Ramana, P.V.; Kumar, G.S.; Sylvia, L.R.; Sumalatha, J.; Reddy, S.A. Fine Ultrasmall Copper Nanoparticle (UCuNPs) Synthesis by Using *Terminalia bellirica* Fruit Extract and Its Antimicrobial Activity. *J. Clust. Sci.* **2016**, *27*, 155–168. [CrossRef]

[95] Wu, S.; Rajeshkumar, S.; Madasamy, M.; Mahendran, V. Green Synthesis of Copper Nanoparticles Using *Cissus vitiginea* and Its Antioxidant and Antibacterial Activity against Urinary Tract Infection Pathogens. *Artif. Cells Nanomed. Biotechnol.* **2020**, *48*, 1153–1158. [CrossRef]

[96] Petla, R.K.; Vivekanandhan, S.; Misra, M.; Mohanty, A.K.; Satyanarayana, N. Soybean (*Glycine max*) Leaf Extract Based Green Synthesis of Palladium Nanoparticles. *J. Biomater. Nanobiotechnol.* **2011**, *3*, 14–19. [CrossRef]

[97] Fahmy, S.A.; Fawzy, I.M.; Saleh, B.M.; Issa, M.Y.; Bakowsky, U.; Azzazy, H.M.E.-S. Green Synthesis of Platinum and Palladium Nanoparticles Using *Peganum harmala* L. Seed Alkaloids: Biological and Computational Studies. *Nanomaterials* **2021**, *11*, 965. [CrossRef] [PubMed]

[98] Molaie, R.; Farhadi, K.; Forough, M.; Hajizadeh, S. Green Biological Fabrication and Characterization of Highly Monodisperse Palladium Nanoparticles Using *Pistacia atlantica* Fruit Broth. *J. Nanostruct.* **2018**, 47–54. [CrossRef]

[99] Vinodhini, S.; Vithiya, B.S.M.; Prasad, T.A.A. Green Synthesis of Palladium Nanoparticles Using Aqueous Plant Extracts and Its Biomedical Applications. *J. King Saud Univ. Sci.* **2022**, *34*, 102017. [CrossRef]

[100] Eltaweil, A.S.; Fawzy, M.; Hosny, M.; El-Monaem, E.M.A.; Tamer, T.M.; Omer, A.M. Green Synthesis of Platinum Nanoparticles Using *Atriplex halimus* Leaves for Potential Antimicrobial, Antioxidant, and Catalytic Applications. *Arab. J. Chem.* **2022**, *15*, 103517. [CrossRef]

[101] Kumar, P.V.; Kala, S.M.J.; Prakash, K. Green Synthesis Derived Pt-Nanoparticles Using *Xanthium strumarium* Leaf Extract and Their Biological Studies. *J. Environ. Chem. Eng.* **2019**, *7*, 103146. [CrossRef]

[102] Liu, L.; Jing, Y.; Guo, A.; Li, X.; Li, Q.; Liu, W.; Zhang, X. Biosynthesis of Platinum Nanoparticles with *Cordyceps* Flower Extract: Characterization, Antioxidant Activity and Antibacterial Ac-

tivity. *Nanomaterials* **2022**, *12*, 1904. [CrossRef] [PubMed]

[103] Bukhari, A.; Ijaz, I.; Gilani, E.; Nazir, A.; Zain, H.; Saeed, R.; Alarfaji, S.S.; Hussain, S.; Aftab, R.; Naseer, Y. Green Synthesis of Metal and Metal Oxide Nanoparticles Using Different Plants' Parts for Antimicrobial Activity and Anticancer Activity: A Review Article. *Coatings* **2021**, *11*, 1374. [CrossRef]

[104] Devabalan, I.; Nambiar, A.; Yadav, A. Synthesis and Characterization of Nanoparticle Enhanced Biodiesel Using *Azadirachta indica* (Neem) Leaf Extract. In *E3S Web of Conferences*; EDP Sciences: Les Ulis, France, 2024; Volume 511, p. 01022. [CrossRef]

[105] Zhang, Y.; Cheng, S.; Jia, H.; Zhou, J.; Xi, J.; Wang, J.; Chen, X.; Wu, L. Green Synthesis of Platinum Nanoparticles by *Nymphaea tetragona* Flower Extract and Their Skin Lightening, Antiaging Effects. *Arab. J. Chem.* **2023**, *16*, 104391. [CrossRef]

[106] Rajeshkumar, S.; Bharath, L. Mechanism of Plant-Mediated Synthesis of Silver Nanoparticles–A Review on Biomolecules Involved, Characterisation and Antibacterial Activity. *Chem. Interact.* **2017**, *273*, 219–227. [CrossRef]

[107] Jeyaraj, M.; Rajesh, M.; Arun, R.; MubarakAli, D.; Sathishkumar, G.; Sivanandhan, G.; Dev, G.K.; Manickavasagam, M.; Premkumar, K.; Thajuddin, N.; et al. An Investigation on the Cytotoxicity and Caspase-Mediated Apoptotic Effect of Biologically Synthesized Silver Nanoparticles Using *Podophyllum hexandrum* on Human Cervical Carcinoma Cells. *Colloids Surf. B Biointerfaces* **2013**, *102*, 708–717. [CrossRef]

[108] Larue, C.; Castillo-Michel, H.; Sobanska, S.; Cécillon, L.; Bureau, S.; Barthès, V.; Ouerdane, L.; Carrière, M.; Sarret, G. Foliar Exposure of the Crop *Lactuca sativa* to Silver Nanoparticles: Evidence for Internalization and Changes in Ag Speciation. *J. Hazard. Mater.* **2014**, *264*, 98–106. [CrossRef]

[109] Khosravi, N.; Charehgani, H.; Abdollahi, M.; Rajabi, H.R. Green Synthesized Silver Nanoparticles Using *Malva sylvestris* as a Potential Management Strategy for Root-Knot Nematode *Meloidogyne javanica* on Tomato *Solanum lycopersicum*. *J. Crop Prot.* **2023**, *12*, 349–363. [CrossRef]

[110] Onitsuka, S.; Hamada, T.; Okamura, H. Preparation of Antimicrobial Gold and Silver Nanoparticles from Tea Leaf Extracts. *Colloids Surf. B Biointerfaces* **2019**, *173*, 242–248. [CrossRef]

[111] Kordsholie, S.M.M.; Rajabi, H.R.; Chadegani, H. Green Synthesis of Silver Nanoparticle by *Hyoscyamus muticus* L. Extract and Study of Its Effect on Tomato Infected with *Meloidogyne javanica*. *J. Mol. Struct.* **2025**, *1323*, 140605. [CrossRef]

[112] Vijilvani, C.; Bindhu, M.; Frincy, F.; AlSalhi, M.S.; Sabitha, S.; Saravanakumar, K.; Devanesan, S.; Umadevi, M.; Aljaafreh, M.J.; Atif, M. Antimicrobial and Catalytic Activities of Biosynthesized Gold, Silver and Palladium Nanoparticles from *Solanum nigurum* Leaves. *J. Photochem. Photobiol. B Biol.* **2020**, *202*, 111713. [CrossRef] [PubMed]

[113] Huang, W.; Yan, M.; Duan, H.; Bi, Y.; Cheng, X.; Yu, H. Synergistic Antifungal Activity of Green Synthesized Silver Nanoparticles and Epoxiconazole against *Setosphaeria turcica*. *J. Nanomater.* **2020**, *2020*, 9535432. [CrossRef]

[114] Bekhradian, A.; Karami, B.; Rajabi, H.R. Green Synthesis of Silver/Silver Oxide Nanostructures Using the *Malva sylvestris* Extract Prior to Simultaneous Distillation Extraction: Synthesis, Phytochemical and Biological Analysis. *Environ. Sci. Pollut. Res.* **2024**, *31*, 60341–60358. [CrossRef] [PubMed]

[115] Qais, F.A.; Shafiq, A.; Ahmad, I.; Husain, F.M.; Khan, R.A.; Hassan, I. Green Synthesis of Silver Nanoparticles Using *Carum copticum*: Assessment of Its Quorum Sensing and Biofilm Inhibitory Potential against Gram Negative Bacterial Pathogens. *Microb. Pathog.* **2020**, *144*, 104172. [CrossRef]

[116] Odeniyi, M.A.; Okumah, V.C.; Adebayo-Tayo, B.C.; Odeniyi, O.A. Green Synthesis and Cream Formulations of Silver Nanoparticles of *Nauclea latifolia* (African Peach) Fruit Extracts and Evaluation of Antimicrobial and Antioxidant Activities. *Sustain. Chem. Pharm.* **2020**, *15*, 100197. [CrossRef]

[117] Rajabi, H.R.; Deris, H.; Faraji, H.S. A Facile and Green Biosynthesis of Silver Nanostructures by Aqueous Extract of *Suaeda acuminata* after Microwave Assisted Extraction. *Nanochemistry Res.* **2016**, *1*, 177–182. [CrossRef]

[118] Patil, T.P.; Vibhute, A.A.; Patil, S.L.; Dongale, T.D.; Tiwari, A.P. Green Synthesis of Gold Nanoparticles via *Capsicum annum* Fruit Extract: Characterization, Antiangiogenic, Antioxidant and Anti-Inflammatory Activities. *Appl. Surf. Sci. Adv.* **2023**, *13*, 100372. [CrossRef]

[119] Fouda, A.; Eid, A.M.; Guibal, E.; Hamza, M.F.; Hassan, S.E.-D.; Alkhalifah, D.H.M.; El-Hossary, D. Green Synthesis of Gold Nanoparticles by Aqueous Extract of *Zingiber officinale*: Characterization and Insight into Antimicrobial, Antioxidant, and *In Vitro* Cytotoxic Activities. *Appl. Sci.* **2022**, *12*, 12879. [CrossRef]

[120] Ahmad, S.; Ahmad, S.; Xu, Q.; Khan, I.; Cao, X.; Yang, R.; Yan, H. Green Synthesis of Gold and Silver Nanoparticles Using Crude Extract of *Aconitum violaceum* and Evaluation of Their Antibacterial, Antioxidant and Photocatalytic Activities. *Front. Bioeng. Biotechnol.* **2024**, *11*, 1320739. [CrossRef]

[121] Xu, V.W.; Nizami, M.Z.I.; Yin, I.X.; Yu, O.Y.; Lung, C.Y.K.; Chu, C.H. Application of Copper Nanoparticles in Dentistry. *Nanomaterials* **2022**, *12*, 805. [CrossRef]

[122] Nguyen, N.T.T.; Nguyen, L.M.; Nguyen, T.T.T.; Nguyen, T.T.; Nguyen, D.T.C.; Van Tran, T. Formation, Antimicrobial Activity, and Biomedical Performance of Plant-Based Nanoparticles: A Review. *Environ. Chem. Lett.* **2022**, *20*, 2531–2571. [CrossRef] [PubMed]

[123] Mehdizadeh, T.; Zamani, A.; Froushani, S.M.A. Preparation of Cu Nanoparticles Fixed on Cellulosic Walnut Shell Material and Investigation of Its Antibacterial, Antioxidant and Anticancer Effects. *Heliyon* **2020**, *6*, e03528. [CrossRef]
[124] Mali, S.C.; Dhaka, A.; Githala, C.K.; Trivedi, R. Green Synthesis of Copper Nanoparticles Using *Celastrus paniculatus* Willd. Leaf Extract and Their Photocatalytic and Antifungal Properties. *Biotechnol. Rep.* **2020**, *27*, e00518. [CrossRef]
[125] Sharma, P.; Pant, S.; Poonia, P.; Kumari, S.; Dave, V.; Sharma, S. Green Synthesis of Colloidal Copper Nanoparticles Capped with *Tinospora cordifolia* and Its Application in Catalytic Degradation in Textile Dye: An Ecologically Sound Approach. *J. Inorg. Organomet. Polym. Mater.* **2018**, *28*, 2463–2472. [CrossRef]
[126] Sattar, Z.A.; Mohammed, A.M.; Khalaf, Y.H. Green Synthesis of *Curcuma longa*-Mediated Palladium Nanoparticles as Antioxidant, Antimicrobial, and Anticancer Agents. *Results Chem.* **2024**, *9*, 101675. [CrossRef]
[127] Bathula, C.K.S.; Kumar, K.A.; Yadav, H.; Ramesh, S.; Shinde, S.; Shrestha, N.K.; Mallikarjuna, K.; Kim, H. Ultrasonically Driven Green Synthesis of Palladium Nanoparticles by *Coleus amboinicus* for Catalytic Reduction and Suzuki-Miyaura Reaction. *Colloids Surf. B Biointerfaces* **2020**, *192*, 111026. [CrossRef] [PubMed]
[128] Puja, P.; Kumar, P. A Perspective on Biogenic Synthesis of Platinum Nanoparticles and Their Biomedical Applications. *Spectrochim. Acta Part A Mol. Biomol. Spectrosc.* **2019**, *211*, 94–99. [CrossRef] [PubMed]
[129] Şahin, B.; Aygün, A.; Gündüz, H.; Şahin, K.; Demir, E.; Akocak, S.; Şen, F. Cytotoxic Effects of Platinum Nanoparticles Obtained from Pomegranate Extract by the Green Synthesis Method on the MCF-7 Cell Line. *Colloids Surf. B Biointerfaces* **2018**, *163*, 119–124. [CrossRef]
[130] Idris, D.S.; Roy, A. Synthesis of Bimetallic Nanoparticles and Applications—An Updated Review. *Crystals* **2023**, *13*, 637. [CrossRef]
[131] Malik, M.A.; Albeladi, S.S.; Al-Maaqar, S.M.; Alshehri, A.A.; Al-Thabaiti, S.A.; Khan, I.; Kamli, M.R. Biosynthesis of Novel Ag-Cu Bimetallic Nanoparticles from Leaf Extract of *Salvia officinalis* and Their Antibacterial Activity. *Life* **2023**, *13*, 653. [CrossRef]
[132] Providence, B.A.; Chinyere, A.A.; Ayi, A.A.; Charles, O.O.; Elijah, T.A.; Ayomide, H.L. Green Synthesis of Silver Monometallic and Copper-Silver Bimetallic Nanoparticles Using *Kigelia africana* Fruit Extract and Evaluation of Their Antimicrobial Activities. *Int. J. Phys. Sci.* **2018**, *13*, 24–32. [CrossRef]
[133] Prasad, C.; Sreenivasulu, K.; Gangadhara, S.; Venkateswarlu, P. Bio Inspired Green Synthesis of Ni/Fe3O4 Magnetic Nanoparticles Using *Moringa oleifera* Leaves Extract: A Magnetically Recoverable Catalyst for Organic Dye Degradation in Aqueous Solution. *J. Alloys Compd.* **2017**, *700*, 252–258. [CrossRef]
[134] Luo, F.; Yang, D.; Chen, Z.; Megharaj, M.; Naidu, R. One-Step Green Synthesis of Bimetallic Fe/Pd Nanoparticles Used to Degrade Orange II. *J. Hazard. Mater.* **2016**, *303*, 145–153. [CrossRef]
[135] Mamatha, G.; Rajulu, A.V.; Madhukar, K. In Situ Generation of Bimetallic Nanoparticles in Cotton Fabric Using Aloe Vera Leaf Extract, as a Reducing Agent. *J. Nat. Fibers* **2020**, *17*, 1121–1129. [CrossRef]
[136] Venkatesan, P.; Santhanalakshmi, J. Synthesis, Characterization and Catalytic Activity of Trimetallic Nanoparticles in the Suzuki C–C Coupling Reaction. *J. Mol. Catal. A Chem.* **2010**, *326*, 99–106. [CrossRef]
[137] Alshehri, A.A.; Malik, M.A. Facile One-Pot Biogenic Synthesis of Cu-Co-Ni Trimetallic Nanoparticles for Enhanced Photocatalytic Dye Degradation. *Catalysts* **2020**, *10*, 1138. [CrossRef]
[138] El-Sawaf, A.K.; El-Moslamy, S.H.; Kamoun, E.A.; Hossain, K. Green Synthesis of Trimetallic CuO/Ag/ZnO Nanocomposite Using *Ziziphus spina-christi* Plant Extract: Characterization, Statistically Experimental Designs, and Antimicrobial Assessment. *Sci. Rep.* **2024**, *14*, 19718. [CrossRef] [PubMed]
[139] Roy, A.; Kunwar, S.; Bhusal, U.; Alghamdi, S.; Almehmadi, M.; Alhuthali, H.M.; Allahyani, M.; Hossain, J.; Hasan, A.; Sarker, M.R.; et al. Bio-Fabrication of Trimetallic Nanoparticles and Their Applications. *Catalysts* **2023**, *13*, 321. [CrossRef]
[140] Mohammed, N.M.S.; Idrees, S.A. Green Synthesis of Co-Zn-Ni Trimetallic Oxide Nanoparticles Using *Cicer arietinum* Leaf Extract and Their Antibiofilm Activity: Experimental and Computational Study. *Mater. Sci. Eng. B* **2024**, *310*, 117681. [CrossRef]
[141] Farooq, U.; Zahra, S.T.; Najeeb, J.; Naseem, K.; Khan, M.E.; Ali, W.; Alomar, M.S.; Ali, S.K.; Hassan, M.; Al Zoubi, W.; et al. Harnessing the Potential of Green Synthesized Co-Fe-ZnS Nanocomposites for Successive Solar-Driven Degradation of Amoxicillin, Hydrogen Production, and CO_2 Reduction: Optimization of Reaction Parameters by Response Surface Methodology. *Sustain. Mater. Technol.* **2025**, *44*, e01377. [CrossRef]
[142] Vaseghi, Z.; Tavakoli, O.; Nematollahzadeh, A. Rapid Biosynthesis of Novel Cu/Cr/Ni Trimetallic Oxide Nanoparticles with Antimicrobial Activity. *J. Environ. Chem. Eng.* **2018**, *6*, 1898–1911. [CrossRef]
[143] Kannaiyan, S.K.; Rengaraj, R.; Gayathri, P.K.; Lavanya, G.; Hemapriya, D. Antimicrobial Activity of Green Synthesized Trimetallic Oxide Ni/Cr/Cu Nanoparticles. *J. Niger. Soc. Phys. Sci.* **2021**, 144–147. [CrossRef]
[144] Hussein, S.; Mahmoud, A.M.; Elgebaly, H.A.; Hendawy, O.M.; Hassanein, E.H.M.; Moustafa, S.M.N.; Alotaibi, N.F.; Nassar, A.M. Green Synthesis of

Trimetallic Nanocomposite (Ru/Ag/Pd)-Np and Its *In Vitro* Antimicrobial and Anticancer Activities. *J. Chem.* **2022**, *2022*, 4593086. [CrossRef]

[145] Radhakrishnan, R.; Srinivasan, S. Plant Mediated Synthesis Cu-Ag-Ru Trimetallic Nanoparticles Using *Andrographis paniculata* Extract: Antibacterial, Anticancer and Photocatalytic Activities. *Orient. J. Chem.* **2024**, *40*. [CrossRef]

[146] Ashour, M.; Mansour, A.T.; Abdelwahab, A.M.; Alprol, A.E. Metal Oxide Nanoparticles' Green Synthesis by Plants: Prospects in Phyto- and Bioremediation and Photocatalytic Degradation of Organic Pollutants. *Processes* **2023**, *11*, 3356. [CrossRef]

[147] Alomar, M.S.; Farooq, U.; Khan, M.E.; Ali, S.K.; Mohammad, A.; Zakri, W. Photo-Induced Degradation of Sulfamerazine Using Green-Synthesized Thermally Stable Novel OE/PE-γ-Al_2O_3 Nanoparticles and the Formulation of Highly Selective CO Formation Through CO_2 Photoreduction: Reaction Kinetics using RSM-CCD Model. *Water Air Soil. Pollut.* **2025**, *236*, 753. [CrossRef]

[148] Huo, Y.; Wu, Z.; Yang, Y.; Dong, B.; Chang, Z. Enhanced Photocatalytic CO_2 Reduction with Incorporation of WO_3 Cocatalyst in g-C_3N_4–TiO_2 Heterojunction. *Molecules* **2025**, *30*, 2317. [CrossRef] [PubMed]

[149] Ishak, N.A.I.M.; Kamarudin, S.K.; Timmiati, S.N. Green Synthesis of Metal and Metal Oxide Nanoparticles via Plant Extracts: An Overview. *Mater. Res. Express* **2019**, *6*, 112004. [CrossRef]

[150] Alhalili, Z. Green Synthesis of Copper Oxide Nanoparticles CuO NPs from *Eucalyptus globulus* Leaf Extract: Adsorption and Design of Experiments. *Arab. J. Chem.* **2022**, *15*, 103739. [CrossRef]

[151] Nzilu, D.M.; Madivoli, E.S.; Makhanu, D.S.; Wanakai, S.I.; Kiprono, G.K.; Kareru, P.G. Green Synthesis of Copper Oxide Nanoparticles and Its Efficiency in Degradation of Rifampicin Antibiotic. *Sci. Rep.* **2023**, *13*, 14030. [CrossRef]

[152] Priya, M.; Venkatesan, R.; Deepa, S.; Sana, S.S.; Arumugam, S.; Karami, A.M.; Vetcher, A.A.; Kim, S.-C. Green Synthesis, Characterization, Antibacterial, and Antifungal Activity of Copper Oxide Nanoparticles Derived from *Morinda citrifolia* Leaf Extract. *Sci. Rep.* **2023**, *13*, 18838. [CrossRef]

[153] Mengesha, S.M.; Abebe, G.M.; Habtemariam, T.H. Biosynthesis of CuO Nanoparticle Using Leaf Extracts of *Ocimum lamiifolium* Hochst. ex Benth and *Withania somnifera* (L) Dunal for Antibacterial Activity. *Sci. Rep.* **2024**, *14*, 23870. [CrossRef] [PubMed]

[154] Siddique, M.H.; Sadia, M.; Muzammil, S.; Saqalein, M.; Ashraf, A.; Hayat, S.; Saba, S.; Khan, A.M.; Hashem, A.; Avila-Qezada, G.D.; et al. Biofabrication of Copper Oxide Nanoparticles Using *Dalbergia sisso* Leaf Extract for Antibacterial, Antibiofilm and Antioxidant Activities. *Sci. Rep.* **2024**, *14*, 31867. [CrossRef] [PubMed]

[155] Shabbir, M.A.; Naveed, M.; Rehman, S.U.; Ain, N.U.; Aziz, T.; Alharbi, M.; Alsahammari, A.; Alasmari, A.F. Synthesis of Iron Oxide Nanoparticles from *Madhuca indica* Plant Extract and Assessment of Their Cytotoxic, Antioxidant, Anti-Inflammatory, and Anti-Diabetic Properties via Different Nanoinformatics Approaches. *ACS Omega* **2023**, *8*, 33358–33366. [CrossRef]

[156] Buarki, F.; AbuHassan, H.; Al Hannan, F.; Henari, F.Z. Green Synthesis of Iron Oxide Nanoparticles Using *Hibiscus rosa sinensis* Flowers and Their Antibacterial Activity. *J. Nanotechnol.* **2022**, *2022*, 5474645. [CrossRef]

[157] Lakshminarayanan, S.; Shereen, M.F.; Niraimathi, K.L.; Brindha, P.; Arumugam, A. One-Pot Green Synthesis of Iron Oxide Nanoparticles from *Bauhinia tomentosa*: Characterization and Application towards Synthesis of 1,3 Diolein. *Sci. Rep.* **2021**, *11*, 8643. [CrossRef]

[158] Sundararaman, S.; Karthikeyan, M.; Kumar, J.A.; Deivasigamani, P.; Soosai, M.R.; Ramaraja, A.; Sahana, S.; Thamer, B.M.; El-Newehy, M.H.; Rajasimman, M.; et al. Facile Synthesis of Iron Nanoparticles from *Camellia sinensis* Leaves Catalysed for Biodiesel Synthesis from *Azolla filiculoides*. *Sci. Rep.* **2024**, *14*, 12818. [CrossRef]

[159] Bhuiyan, S.H.; Miah, M.Y.; Paul, S.C.; Das Aka, T.; Saha, O.; Rahaman, M.; Sharif, J.I.; Habiba, O.; Ashaduzzaman. Green Synthesis of Iron Oxide Nanoparticle Using *Carica papaya* Leaf Extract: Application for Photocatalytic Degradation of Remazol Yellow RR Dye and Antibacterial Activity. *Heliyon* **2020**, *6*, e04603. [CrossRef]

[160] Adhikari, A.; Chhetri, K.; Acharya, D.; Pant, B.; Adhikari, A. Green Synthesis of Iron Oxide Nanoparticles Using *Psidium guajava* L. Leaves Extract for Degradation of Organic Dyes and Anti-Microbial Applications. *Catalysts* **2022**, *12*, 1188. [CrossRef]

[161] Miri, A.; Khatami, M.; Sarani, M. Biosynthesis, Magnetic and Cytotoxic Studies of Hematite Nanoparticles. *J. Inorg. Organomet. Polym. Mater.* **2020**, *30*, 767–774. [CrossRef]

[162] Rajeshkumar, S.; Parameswari, R.P.; Sandhiya, D.; Al-Ghanim, K.A.; Nicoletti, M.; Govindarajan, M. Green Synthesis, Characterization and Bioactivity of *Mangifera indica* Seed-Wrapped Zinc Oxide Nanoparticles. *Molecules* **2023**, *28*, 2818. [CrossRef] [PubMed]

[163] Jan, H.; Shah, M.; Andleeb, A.; Faisal, S.; Khattak, A.; Rizwan, M.; Drouet, S.; Hano, C.; Abbasi, B.H. Plant-Based Synthesis of Zinc Oxide Nanoparticles (ZnO-NPs) Using Aqueous Leaf Extract of *Aquilegia pubiflora*: Their Antiproliferative Activity against HepG2 Cells Inducing Reactive Oxygen Species and Other *In Vitro* Properties. *Oxidative Med. Cell. Longev.* **2021**, *2021*, 4786227. [CrossRef]

[164] Jobie, F.N.; Ranjbar, M.; Moghaddam, A.H.; Kiani, M. Green Synthesis of Zinc Oxide Nanoparticles Using *Amygdalus scoparia* Spach Stem Bark Extract and Their Applications as an Alternative Antimicrobial, Anticancer, and Anti-Diabetic Agent. *Adv. Powder Technol.* **2021**, *32*, 2043–2052. [CrossRef]

[165] Chandra, H.; Patel, D.; Kumari, P.; Jangwan, J.; Yadav, S. Phyto-Mediated Synthesis of Zinc Oxide Nanoparticles of *Berberis aristata*: Characterization, Antioxidant Activity and Antibacterial Activity with Special Reference to Urinary Tract Pathogens. *Mater. Sci. Eng. C* **2019**, *102*, 212–220. [CrossRef]

[166] Faisal, S.; Jan, H.; Shah, S.A.; Shah, S.; Khan, A.; Akbar, M.T.; Rizwan, M.; Jan, F.; Wajidullah; Akhtar, N.; et al. Green Synthesis of Zinc Oxide (ZnO) Nanoparticles Using Aqueous Fruit Extracts of *Myristica fragrans*: Their Characterizations and Biological and Environmental Applications. *ACS Omega* **2021**, *6*, 9709–9722. [CrossRef]

[167] Bopape, D.A.; Tetana, Z.N.; Mabuba, N.; Motaung, D.E.; Hintsho-Mbita, N.C. Biosynthesis of TiO_2 Nanoparticles Using *Commelina benghalensis* for the Photodegradation of Methylene Blue Dye and Antibiotics: Effect of Plant Concentration. *Results Chem.* **2023**, *5*, 100825. [CrossRef]

[168] Mbenga, Y.; Adeyemi, J.O.; Mthiyane, D.M.; Singh, M.; Onwudiwe, D.C. Green Synthesis, Antioxidant and Anticancer Activities of TiO_2 Nanoparticles Using Aqueous Extract of *Tulbaghia violacea*. *Results Chem.* **2023**, *6*, 101007. [CrossRef]

[169] Arabi, N.; Kianvash, A.; Hajalilou, A.; Abouzari-Lotf, E.; Abbasi-Chianeh, V. A Facile and Green Synthetic Approach toward Fabrication of Alcea- and Thyme-Stabilized TiO_2 Nanoparticles for Photocatalytic Applications. *Arab. J. Chem.* **2020**, *13*, 2132–2141. [CrossRef]

[170] Saka, A.; Shifera, Y.; Jule, L.T.; Badassa, B.; Nagaprasad, N.; Shanmugam, R.; Dwarampudi, L.P.; Seenivasan, V.; Ramaswamy, K. Biosynthesis of TiO_2 Nanoparticles by Caricaceae (Papaya) Shell Extracts for Antifungal Application. *Sci. Rep.* **2022**, *12*, 15960. [CrossRef]

[171] Al-Shabib, N.A.; Husain, F.M.; Qais, F.A.; Ahmad, N.; Khan, A.; Alyousef, A.A.; Arshad, M.; Noor, S.; Khan, J.M.; Alam, P.; et al. Phyto-Mediated Synthesis of Porous Titanium Dioxide Nanoparticles from *Withania somnifera* Root Extract: Broad-Spectrum Attenuation of Biofilm and Cytotoxic Properties against HepG2 Cell Lines. *Front. Microbiol.* **2020**, *11*, 1680. [CrossRef]

[172] Swathi, N.; Sandhiya, D.; Rajeshkumar, S.; Lakshmi, T. Green Synthesis of Titanium Dioxide Nanoparticles Using *Cassia fistula* and Its Antibacterial Activity. *Int. J. Res. Pharm. Sci.* **2019**, *10*, 856–860. [CrossRef]

[173] Mohany, M.; Ullah, I.; Fozia, F.; Aslam, M.; Ahmad, I.; Sharifi-Rad, M.; Al-Rejaie, S.S.; Zaghloul, N.S.S.; Ahmad, S.; Aboul-Soud, M.A.M. Biofabrication of Titanium Dioxide Nanoparticles Catalyzed by *Solanum surattense*: Characterization and Evaluation of Their Antiepileptic and Cytotoxic Activities. *ACS Omega* **2023**, *8*, 16948–16955. [CrossRef]

[174] Dinga, E.; Ekennia, A.; Ogbonna, C.U.; Udu, D.A.; Mthiyane, D.M.N.; Marume, U.; Onwudiwe, D.C. Phyto-Mediated Synthesis of MgO Nanoparticles Using *Melia azedarach* Seed Extract: Larvicidal and Antioxidant Activities. *Sci. Afr.* **2022**, *17*, e01366. [CrossRef]

[175] Younis, I.Y.; El-Hawary, S.S.; Eldahshan, O.A.; Abdel-Aziz, M.M.; Ali, Z.Y. Green Synthesis of Magnesium Nanoparticles Mediated from *Rosa floribunda* Charisma Extract and Its Antioxidant, Antiaging and Antibiofilm Activities. *Sci. Rep.* **2021**, *11*, 16868. [CrossRef]

[176] Rotti, R.B.; Sunitha, D.V.; Manjunath, R.; Roy, A.; Mayegowda, S.B.; Gnanaprakash, A.P.; Alghamdi, S.; Almehmadi, M.; Abdulaziz, O.; Allahyani, M.; et al. Green Synthesis of MgO Nanoparticles and Its Antibacterial Properties. *Front. Chem.* **2023**, *11*, 1143614. [CrossRef]

[177] Abinaya, S.; Kavitha, H.P. Magnesium Oxide Nanoparticles: Effective Antilarvicidal and Antibacterial Agents. *ACS Omega* **2023**, *8*, 5225–5233. [CrossRef]

[178] Venkatachalam, A.; Jesuraj, J.P.; Sivaperuman, K. *Moringa oleifera* Leaf Extract-Mediated Green Synthesis of Nanostructured Alkaline Earth Oxide (MgO) and Its Physicochemical Properties. *J. Chem.* **2021**, *2021*, 4301504. [CrossRef]

[179] Bibi, H.; Ahmad, M.; Osman, A.I.; Alsahli, A.A.; Munir, M.; Al-Muhtaseb, A.H.; Rooney, D.W.; Sultana, S. Green Synthesis of Highly Active and Recyclable Chromium Oxide Nanocatalyst for Biodiesel Production from Novel Nonedible Oil Seeds. *GCB Bioenergy* **2024**, *16*, e13140. [CrossRef]

[180] Muhaymin, A.; Mohamed, H.E.A.; Hkiri, K.; Safdar, A.; Azizi, S.; Maaza, M. Green Synthesis of Magnesium Oxide Nanoparticles Using *Hyphaene thebaica* Extract and Their Photocatalytic Activities. *Sci. Rep.* **2024**, *14*, 20135. [CrossRef]

[181] Nasrollahzadeh, M.; Sajadi, S.M.; Rostami-Vartooni, A. Green Synthesis of CuO Nanoparticles by Aqueous Extract of *Anthemis nobilis* Flowers and Their Catalytic Activity for the A3 Coupling Reaction. *J. Colloid Interface Sci.* **2015**, *459*, 183–188. [CrossRef] [PubMed]

[182] Andualem, W.W.; Sabir, F.K.; Mohammed, E.T.; Belay, H.H.; Gonfa, B.A. Synthesis of Copper Oxide Nanoparticles Using Plant Leaf Extract of *Catha edulis* and Its Antibacterial Activity. *J. Nanotechnol.* **2020**, *2020*, 2932434. [CrossRef]

[183] Abosede, O.O.; Obiyenwa, G.K. Green Synthesis of Copper Oxide Nanoparticles Using *Justicia carnea*. *Int. J. Chem. Stud.* **2022**, *10*, 2932434. [CrossRef]

[184] Afzal, G.; Jamal, A.; Kiran, S.; Mustafa, G.; Mehmood, T.; Ahmad, F.; Saeed, S.; Ali, A.; Naz, N.; Zehra, S.; et al. Copper Oxide Nanoparticles Synthesis Using *Aerva javanica* and Their Antimicrobial Activities. *J. Anim. Plant Sci.* **2022**, *32*, 1403–1411. [CrossRef]

[185] Sukumar, S.; Rudrasenan, A.; Nambiar, D.P. Green-Synthesized Rice-Shaped Copper Oxide Nanoparticles Using *Caesalpinia bonducella* Seed Extract and Their Applications. *ACS Omega* **2020**, *5*, 1040–1051. [CrossRef]

[186] Atri, A.; Echabaane, M.; Bouzidi, A.; Harabi, I.; Soucase, B.M.; Ben Chaâbane, R. Green Synthesis of Copper Oxide Nanoparticles Using *Ephedra alata* Plant Extract and a Study of Their Antifungal, Antibacterial Activity and Photocatalytic Performance under Sunlight. *Heliyon* **2023**, *9*, e13484. [CrossRef]

[187] Al-Darwesh, M.Y.; Ibrahim, S.S.; Mohammed, M.A. A Review on Plant Extract Mediated Green Synthesis of Zinc Oxide Nanoparticles and Their Biomedical Applications. *Results Chem.* **2024**, *7*, 101368. [CrossRef]

[188] Manojkumar, U.; Kaliannan, D.; Srinivasan, V.; Balasubramanian, B.; Kamyab, H.; Mussa, Z.H.; Palaniyappan, J.; Mesbah, M.; Chelliapan, S.; Palaninaicker, S. Green Synthesis of Zinc Oxide Nanoparticles Using *Brassica oleracea* var. *botrytis* Leaf Extract: Photocatalytic, Antimicrobial and Larvicidal Activity. *Chemosphere* **2023**, *323*, 138263. [CrossRef] [PubMed]

[189] Idris, N.A.; Yusoff, H.M.; Idris, N.H.; Badar, N.; Elong, K.; Muhamad, S.U.; Yusoff, N.F.M.; Wai, C.P. Green Synthesis of Zinc Oxide Nanoparticles Using Leaves Extract of Mariposa *Christia vespertilionis* and Its Potential as Anode Materials in Sodium-Ion Batteries (SIBs). *Arab. J. Sci. Eng.* **2024**, *49*, 623–635. [CrossRef]

[190] Karimzadeh, M.R.; Soltanian, S.; Sheikhbahaei, M.; Mohamadi, N. Characterization and Biological Activities of Synthesized Zinc Oxide Nanoparticles Using the Extract of *Acantholimon serotinum*. *Green Process. Synth.* **2020**, *9*, 722–733. [CrossRef]

[191] Sana, S.S.; Kumbhakar, D.V.; Pasha, A.; Pawar, S.C.; Grace, A.N.; Singh, R.P.; Nguyen, V.-H.; Van Le, Q.; Peng, W. *Crotalaria verrucosa* Leaf Extract Mediated Synthesis of Zinc Oxide Nanoparticles: Assessment of Antimicrobial and Anticancer Activity. *Molecules* **2020**, *25*, 4896. [CrossRef]

[192] Emamifard, Z.; Rajabi, H.R. Green Synthesis of Hematite Nanoparticles Using Aqueous Extract of *Teucrium polium* after Microwave-Assisted Extraction: Synthesis, Characterization and Evaluation of Some Biological Activities. *J. Biotech. Res.* **2021**, *5*, 15–22. [View Online]

[193] Aida, M.; Alonizan, N.; Zarrad, B.; Hjiri, M. Green Synthesis of Iron Oxide Nanoparticles Using *Hibiscus* Plant Extract. *J. Taibah Univ. Sci.* **2023**, *17*, 2221827. [CrossRef]

[194] Desalegn, B.; Megharaj, M.; Chen, Z.; Naidu, R. Green Synthesis of Zero Valent Iron Nanoparticle Using Mango Peel Extract and Surface Characterization Using XPS and GC-MS. *Heliyon* **2019**, *5*, e01750. [CrossRef]

[195] Rostamizadeh, E.; Iranbakhsh, A.; Majd, A.; Arbabian, S.; Mehregan, I. Green Synthesis of Fe2O3 Nanoparticles Using Fruit Extract of *Cornus mas* L. and Its Growth-Promoting Roles in Barley. *J. Nanostruct. Chem.* **2020**, *10*, 125–130. [CrossRef]

[196] Jamzad, M.; Bidkorpeh, M.K. Green Synthesis of Iron Oxide Nanoparticles by the Aqueous Extract of *Laurus nobilis* L. Leaves and Evaluation of the Antimicrobial Activity. *J. Nanostruct. Chem.* **2020**, *10*, 193–201. [CrossRef]

[197] Langa, C.; Hintsho-Mbita, N.C. Plant and Bacteria Mediated Synthesis of TiO_2 NPs for Dye Degradation in Water. A Review. *Chem. Phys. Impact* **2023**, *7*, 100293. [CrossRef]

[198] Rathi, V.H.; Jeice, A.R. Green Fabrication of Titanium Dioxide Nanoparticles and Their Applications in Photocatalytic Dye Degradation and Microbial Activities. *Chem. Phys. Impact* **2023**, *6*, 100197. [CrossRef]

[199] Sethy, N.K.; Arif, Z.; Mishra, P.K.; Kumar, P. Green Synthesis of TiO_2 Nanoparticles from *Syzygium cumini* Extract for Photo-Catalytic Removal of Lead (Pb) in Explosive Industrial Wastewater. *Green. Process. Synth.* **2020**, *9*, 171–181. [CrossRef]

[200] Aravind, M.; Amalanathan, M.; Mary, M.S.M. Synthesis of TiO_2 Nanoparticles by Chemical and Green Synthesis Methods and Their Multifaceted Properties. *SN Appl. Sci.* **2021**, *3*, 409. [CrossRef]

[201] Balaraman, P.; Balasubramanian, B.; Liu, W.-C.; Kaliannan, D.; Durai, M.; Kamyab, H.; Alwetaishi, M.; Maluventhen, V.; Ashokkumar, V.; Chelliapan, S.; et al. *Sargassum myriocystum*-Mediated TiO_2-Nanoparticles and Their Antimicrobial, Larvicidal Activities and Enhanced Photocatalytic Degradation of Various Dyes. *Environ. Res.* **2022**, *204*, 112278. [CrossRef] [PubMed]

[202] Radulescu, D.-M.; Surdu, V.-A.; Ficai, A.; Ficai, D.; Grumezescu, A.-M.; Andronescu, E. Green Synthesis of Metal and Metal Oxide Nanoparticles: A Review of the Principles and Biomedical Applications. *Int. J. Mol. Sci.* **2023**, *24*, 15397. [CrossRef]

[203] Zhu, L.; Chen, L.; Gu, J.; Ma, H.; Wu, H. Carbon-Based Nanomaterials for Sustainable Agriculture: Their Application as Light Converters, Nanosensors, and Delivery Tools. *Plants* **2022**, *11*, 511. [CrossRef] [PubMed]

[204] Khan, M.E. State-of-the-Art Developments in Carbon-Based Metal Nanocomposites as a Catalyst: Photocatalysis. *Nanoscale Adv.* **2021**, *3*, 1887–1900. [CrossRef] [PubMed]

[205] Qasim, M.; Clarkson, A.N.; Hinkley, S.F.R. Green Synthesis of Carbon Nanoparticles (CNPs) from Biomass for Biomedical Applications. *Int. J. Mol. Sci.* **2023**, *24*, 1023. [CrossRef] [PubMed]

[206] Ross, S.; Wu, R.-S.; Wei, S.-C.; Ross, G.M.; Chang, H.-T. The Analytical and Biomedical Applications of Carbon Dots and Their Future Theranostic Potential: A Review. *J. Food Drug Anal.* **2020**, *28*, 678–696. [CrossRef]

[207] Liu, K.-K.; Wang, C.-C.; Cheng, C.-L.; Chao, J.-I. Endocytic Carboxylated Nanodiamond for the Labeling and Tracking of Cell Division and Differentiation in Cancer and Stem Cells. *Biomaterials* **2009**, *30*, 4249–4259. [CrossRef]

[208] Perevedentseva, E.; Hong, S.-F.; Huang, K.-J.; Chiang, I.-T.; Lee, C.-Y.; Tseng, Y.-T.; Cheng, C.-L. Nanodiamond Internalization in Cells and the Cell Up-

take Mechanism. *J. Nanoparticle Res.* **2013**, *15*, 1834. [CrossRef]
[209] Ruan, G.; Sun, Z.; Peng, Z.; Tour, J.M. Growth of Graphene from Food, Insects, and Waste. *ACS Nano* **2011**, *5*, 7601–7607. [CrossRef]
[210] Kim, Y.-K.; Kim, M.-H.; Min, D.-H. Biocompatible Reduced Graphene Oxide Prepared by Using Dextran as a Multifunctional Reducing Agent. *Chem. Commun.* **2011**, *47*, 3195–3197. [CrossRef]
[211] Gurunathan, S.; Han, J.W.; Park, J.H.; Eppakayala, V.; Kim, J.-H. *Ginkgo biloba*: A Natural Reducing Agent for the Synthesis of Cytocompatible Graphene. *Int. J. Nanomed.* **2014**, *9*, 363–377. [CrossRef]
[212] Qu, J.; Luo, C.; Cong, Q.; Yuan, X. Recycling of the Hyperaccumulator *Brassica juncea* L.: Synthesis of Carbon Nanotube-Cu/ZnO Nanocomposites. *J. Mater. Cycles Waste Manag.* **2014**, *16*, 162–166. [CrossRef]
[213] Singh, P.; Dan, A.; Kannan, P.P.; Dhanka, M.; Bhatia, D.; Saha, J. Non-Toxic Fabrication of Fluorescent Carbon Nanoparticles from Medicinal Plants/Sources with Their Antioxidant Assay. *arXiv* **2024**, arXiv:2401.10673. [CrossRef]
[214] Tripathi, N.; Pavelyev, V.; Islam, S.S. Synthesis of Carbon Nanotubes Using Green Plant Extract as Catalyst: Unconventional Concept and Its Realization. *Appl. Nanosci.* **2017**, *7*, 557–566. [CrossRef]
[215] Arízaga, G.G.C.; Galván, J.G.Q.; Bail, A.; González, A.L.P.; Nuñez, C.P.; Álvarez, M.Á.L. Green Approach to Synthesize Functional Carbon Nanoparticles at Low Temperature. *Sustain. Chem. Clim. Action* **2022**, *1*, 100002. [CrossRef]
[216] Nadeem, S.; Javed, M.; Iqbal, S.; Mohyuddin, A.; Mahmood, Q.; Abbas, Q.; Alfryyan, N.; Alqahtani, M.D.; Alotaibi, M.T.; Alsaab, H.O.; et al. Facile Synthesis of Catalyst Free Carbon Nanoparticles From the Soot of Natural Oils. *Front. Mater.* **2022**, *9*, 874726. [CrossRef]
[217] Damera, D.P.; Manimaran, R.; Venuganti, V.V.K.; Nag, A. Green Synthesis of Full-Color Fluorescent Carbon Nanoparticles from Eucalyptus Twigs for Sensing the Synthetic Food Colorant and Bioimaging. *ACS Omega* **2020**, *5*, 19905–19918. [CrossRef]
[218] Yildirim, O.; Ozkaya, B. Enhancing Fermentation Yield for Biohydrogen Production Using Eco-Friendly Nickel and Cobalt Ferrite Nanoparticles. *Biomass-Convers. Biorefinery* **2024**, *15*, 26613–26622. [CrossRef]
[219] Guin, M.; Kundu, T.; Singh, R. Applications of Nanotechnology in Biofuel Production. In *Bio-Clean Energy Technologies*; Springer Nature Singapore: Singapore, 2022; Volume 2, pp. 297–332. [CrossRef]
[220] Osman, A.I.; Zhang, Y.; Farghali, M.; Rashwan, A.K.; Eltaweil, A.S.; El-Monaem, E.M.A.; Mohamed, I.M.A.; Badr, M.M.; Ihara, I.; Rooney, D.W.; et al. Synthesis of Green Nanoparticles for Energy, Biomedical, Environmental, Agricultural, and Food Applications: A Review. *Environ. Chem. Lett.* **2024**, *22*, 841–887. [CrossRef]
[221] Zhang, X.; Yan, S.; Tyagi, R.; Surampalli, R. Biodiesel Production from Heterotrophic Microalgae through Transesterification and Nanotechnology Application in the Production. *Renew. Sustain. Energy Rev.* **2011**, *26*, 216–223. [CrossRef]
[222] Qiu, F.; Li, Y.; Yang, D.; Li, X.; Sun, P. Heterogeneous Solid Base Nanocatalyst: Preparation, Characterization and Application in Biodiesel Production. *Bioresour. Technol.* **2022**, *102*, 4150–4156. [CrossRef]
[223] Saka, A.; Enkosa, E.; Jule, L.T.; Nagaprasad, N.; Subramanian, K.; Ramaswamy, K. Biofuel Production from Mango (*Mangifera indica*) Seed Extracts through Zinc Oxide Nanoparticle. *Biomass-Convers. Biorefinery* **2023**, *15*, 22279–22289. [CrossRef]
[224] Arun, S.; Karthik, B.; Yatish, K.; Prashanth, K.; Balakrishna, G.R. Green Synthesis of Copper Oxide Nanoparticles Using the *Bombax ceiba* Plant: Biodiesel Production and Nano-Additive to Investigate Diesel Engine Performance-Emission Characteristics. *Energy* **2022**, *274*, 127345. [CrossRef]
[225] Cholapandian, K.; Gurunathan, B.; Rajendran, N. Investigation of CaO Nanocatalyst Synthesized from *Acalypha indica* Leaves and Its Application in Biodiesel Production Using Waste Cooking Oil. *Fuel* **2021**, *312*, 122958. [CrossRef]
[226] Changmai, B.; Rano, R.; Vanlalveni, C.; Rokhum, S.L. A Novel *Citrus sinensis* Peel Ash Coated Magnetic Nanoparticles as an Easily Recoverable Solid Catalyst for Biodiesel Production. *Fuel* **2024**, *286*, 119447. [CrossRef]
[227] Subramani, K.; Wutthithien, P.; Saha, R.; Lindblad, P.; Incharoensakdi, A. Characterization and Potentiality of Plant-Derived Silver Nanoparticles for Enhancement of Biomass and Hydrogen Production in *Chlorella* sp. under Nitrogen Deprived Condition. *Chemosphere* **2021**, *361*, 142514. [CrossRef] [PubMed]
[228] Bao, Y.; He, J.; Song, K.; Guo, J.; Zhou, X.; Liu, S. Plant-Extract-Mediated Synthesis of Metal Nanoparticles. *J. Chem.* **2023**, *2021*, 6562687. [CrossRef]
[229] Pramanik, A.; Chaudhary, A.A.; Sinha, A.; Chaubey, K.K.; Ashraf, M.S.; Basher, N.S.; Rudayni, H.A.; Dayal, D.; Kumar, S. Nanocatalyst-Based Biofuel Generation: An Update, Challenges and Future Possibilities. *Sustainability* **2023**, *15*, 6180. [CrossRef]